

~~00057~~

0145

8004090 684

CONTENTS

APPENDIX 14

14A ANSWERS TO QUESTIONS

~~00050~~

0146

QUESTION 14A.1 Calculate the minimum shutdown margin for the loss-of-coolant flow and loss-of-electric power transients, using assumptions which result in the most reactive conditions.

ANSWER Minimum Shutdown Margin - Loss of Coolant and Loss of Power

Refer to 14.1.2.6 and 14.1.2.8 The loss-of-coolant flow and the loss-of-electric-power transients are essentially identical in terms of core response. The core coolant temperature rises a few degrees initially and then falls off very slowly, asymptotically approaching a limit of 542 F. The table shows the negative reactivity margin available during the loss-of-coolant-flow transient.

Reactivity Margin During the Loss-of-Coolant-Flow Transient

<u>Time, seconds</u>	<u>Reactivity Margin, % <math>\Delta k/k</math></u>	
	<u>BOL</u>	<u>EOL</u>
10	-5.4	-5.5
100	-5.6	-5.0
Steady state (542 F and equilibrium Xe)	-4.1	-3.4

~~00059~~

0147

QUESTION  
14A.2

Expand the analysis of loss of off-site power with a reactor scram to indicate the long-term consequences. Can the reactor be depressurized so that the low pressure heat removal systems, operative on emergency power, could function? Consider providing means to deliver service water or cooling tower inventory to the hot-well as a means of increasing the available feedwater source.

ANSWER  
Refer to  
14.1.2.8.3 e

The primary method of decay heat removal from the reactor cooling system at temperatures above 250 F is the utilization of one or both of the steam generators. Accordingly, any shutdown condition above 250 F requires a supply of boiler feedwater which must be guaranteed. There is no other method by which the reactor can be depressurized to permit the functioning of the low pressure heat removal systems.

The feedwater normal supply system (3 half capacity condensate pumps, 2 half capacity turbine driven main feedwater pumps) provides this if electrical power is available.

2 |

During "blackout" conditions, either the motor driven or the turbine driven 5% capacity feedwater pumps is capable of pumping against full steam generator pressure. The pumps take suction from the condensate storage tank, or alternatively from the demineralized water storage tank. The motor driven pump will be diesel backed. On loss of off-site power, which is considered a short-term consequence, the reactor would not be depressurized but held at full pressure to effect a quick return to the system as soon as off-site power is re-established.

2 |

~~00000~~

148

QUESTION 14A. 3 Discuss the possibility of control rod ejection due to a rod drive seal or vent failure.

ANSWER The control rod assembly including drive shaft weighs in excess of 250 pounds in water. This assembly has a 2.4-in.<sup>2</sup>, flat projected area which could be available for a piston effect if the pressure in the control rod housing were lower than the pressure in the reactor vessel. A pressure differential in excess of 100 psi would be required to cause outward motion of the control rod.

The possibility of a control rod ejection due to a rod drive seal failure has been evaluated by assuming that the buffer seal assembly offers no resistance to flow from the reactor vessel to the atmosphere. Figure 3.2-65 of the PSAR shows that between the reactor vessel and the upper seal assembly that there are a number of cross-sectional area changes which in effect provide a series of pressure breakdown mechanisms. By utilizing these restricted flow areas, sufficient breakdown of the pressure occurs such that less than 20 lb/sec will flow from the reactor vessel into the rod drive housing. This flow will produce a pressure differential of approximately 20 psi which results in an additional (over operating) upward force on the control rod of only 48 pounds. This force is a factor of 4 below that required to produce control rod motion.

As can be seen on Figure 3.2-65, the vent at the top of the rack housing has a very small cross-sectional area available for leakage flow to the atmosphere in the event of a failure of this component. This 1/4-in. diam vent line has an area of 0.05 in.<sup>2</sup> as compared to 0.975 in.<sup>2</sup> available for supplying flow into the rack housing from the reactor vessel. With this large area difference, a maximum pressure drop of 5.5 psi would be developed across the control rod. This pressure drop is not sufficient to cause control rod motion.

It is therefore concluded that neither a failure of the rod drive seal nor of the vent piping on the rack housing will produce a sufficient pressure differential across the control rod to cause control rod motion, and therefore a rod ejection accident cannot occur as a result of failure of these components.

~~00001~~

0149

QUESTION  
14A.4

Discuss the influence of the void geometry assumed on the calculation of the reactivity inserted due to a positive moderator temperature coefficient during a loss-of-coolant accident. Would a reduced density in the center of the core have more effect on peak temperatures than a uniform decrease in density?

ANSWER  
Refer to  
14.2.2.3.4a

The analysis of the core kinetics during the LOCA has been based on a detailed breakdown of the average channel using coefficients generated by assuming uniform void distribution. The calculation of reactivity effects in a thermal reactor using the assumption of uniformity is a good one if the reactivity has some reasonable distribution through the core. The maximum density variation at core exit at ultimate power is only  $\pm 5$  percent; therefore, the distribution is relatively even. The distribution at mid-core is even closer.

There is no analytical model available for calculating the void fraction as a function of radius and azimuth during a LOCA, nor is there any way of accounting for such a distribution in a kinetics analysis. Since there is such an even distribution of the voids, however, the reactivity feedback is also expected to be uniform. Therefore, the reactivity held in any one fuel assembly (or group) is very low and nearly proportional to its volume fraction in the core. It is concluded, then, that the average channel simulation used by the CHICKEN computer code is an accurate one. The program considers six axial segments in the fuel, clad, and water; and six segments radially in the fuel. The code also weights the reactivity feedback according to the importance of each region. Since the principal voiding effects are occurring in axial dimension, the code does a proper calculation of the feedback.

In the unrealistic case where it is assumed that voiding of many central fuel assemblies occurs, the local flux in this region will tend to increase and decrease relative to the rest of the core. This would be similar in result to a rod ejection accident of very small rod worth. Since the density variation in the radial direction is less than 5 percent, the effect on total reactivity addition and, therefore, on peak temperatures, would be small.

0150

~~00002~~

QUESTION 14A.5 Justify the assumption of a heat transfer coefficient of 20 Btu/hr ft<sup>2</sup> °F in the upper half of core when the core is one-half filled with water after a loss-of-coolant accident.

ANSWER Refer to 14.2.2.3.4 The water coming in through the emergency injection lines from the core flooding tanks very quickly starts to recover the core with borated water. The core at this time still retains a lot of its sensible heat, and is generating heat due to the decay of fission products and other heavy isotopes. When recovery of the core starts, heat is transferred to the water; and after heating to the saturation point, steam is produced. By the time the core is half-covered, the steam production rate is on the order of 200 to 300 lb/sec.

The convective heat transfer coefficient for the variable steam generation rates existing during refilling has been evaluated using the following heat transfer correlation:

$$h_c = 0.023 k/D(R_e)^{0.8}(P_r)^{1/3}$$

Without considering radiation, the  $h_c$  developed for a 200-lb/sec flow ranges from 23 to 30 Btu/hr-ft<sup>2</sup>-F for steam temperatures ranging from 400 to 1,200 F. In the clad temperature range of 1,600 F, radiation from the clad to 800 F steam can contribute approximately another 3 Btu/hr-ft<sup>2</sup>-F.

However, even though the upper part of the core experiences steam cooling, core covering will not terminate at the core midplane. There is enough water in the core flooding tanks to fill the core past the three-quarter point taking no credit for the increase in volume due to steam formation. Thereafter, in less than 30 sec the core will be completely covered, and will remain so due to the action of the high and low pressure injection systems running at two-thirds of their capacity.

0151

~~00003~~

QUESTION  
14A.6

Provide an analysis of the loss-of-coolant accident for a spectrum of break sizes and locations, including those breaks in the emergency core cooling systems which also reduce the injection capability. Include curves of the pressure, water level, and fuel cladding temperature transients for each break size considered. Submit a chart showing the overlap and redundancy in the systems which cover various break sizes. Discuss the following:

- 14A.6.1 A detailed description of how the steam bubble velocity as a function of pressure was determined. Include a description of the physical process occurring in the reactor vessel during blowdown and discuss the limits of applicability of steady-state bubble rise data to blowdown analyses.
- 14A.6.2 A comparison of pressure and water level transients for the variable-bubble-velocity model and the constant-bubble-velocity model for a spectrum of break sizes. In addition, compare these with LOFT semiscale blowdown data with and without internals in place for various break sizes.
- 14A.6.3 How the design of the high pressure injection system is affected by the assumed bubble velocity model.

ANSWER

Refer to  
14.2.2.3.4

Steam Bubble Velocity as a Function of Pressure

In the process of trying to correlate the LOFT semiscale blowdown tests using the FLASH code, it became apparent that the method employed in FLASH to determine the amount of steam-water separation did not adequately describe the phenomena. The variable that determines the amount of steam-water separation in the FLASH program is the steam bubble rise velocity. The original value of the bubble velocity incorporated into FLASH was based on a report by Wilson et al.<sup>1</sup> This report shows experimentally determined terminal velocities of steam bubbles rising through saturated water. Data were obtained for the velocity as a function of void fraction and pressure in two different diameter test vessels. Over the range of pressures considered, the bubble velocity varied between 1 and 7 ft/sec. The authors of FLASH chose a constant value of 2 ft/sec.

For a given void fraction, a plot of the same steam bubble velocity versus pressure data as referenced above shows an increase in velocity with a decrease in pressure. A curve was fitted to the data to obtain the form of the equation.

~~00584~~

0152



This expression was then inserted into the FLASH program in place of the constant 2-ft/sec value. Using the same form of the equation, the coefficients were changed until a bubble velocity was obtained that gave the best fit to the experimental data obtained from the LOFT semiscale blowdown tests without internals in the vessel.

During the depressurization of a high temperature water system, steam bubbles will be formed due to the flashing of the water. The rate of formation of the steam bubbles depends on the heat addition and the rate of depressurization. If the steam bubbles are generated rapidly enough, they will rise, mix and coalesce, and entrain water droplets. If the rate of formation is slow enough, the steam bubbles will be unable to entrain water droplets, and complete separation of the steam and water will occur.

Until recently, only steady-state data on flashing steam-water systems were available. The use of steady-state data is very useful in that certain phenomena can be examined without having perturbations from some other critical parameter. For example, in the case of the bubble velocity experiment, bubble velocities were obtained at different void fractions but at a constant pressure. By making series of tests at different pressures, the pressure effect on the bubble velocity can be more clearly defined.

By making use of this steady-state data together with the transient data currently being obtained by the Phillips Petroleum Company in connection with the LOFT project, better empirical relationships for describing the physical processes can be obtained. As can be seen from the answer to Question 14A.6.2 below, the relationships now being employed are conservative.

14A.6.2 Comparison - Bubble Velocity Models

The variable bubble velocity model has been used to correlate the LOFT semiscale blowdown tests. The only data that have been released that show time-dependent pressure traces are those corresponding to a 100 percent break area and a 6.1 percent break area. These data are for the blowdown tests without the simulated internals installed. Information showing the percent mass remaining 3 min after depressurization has been reported for a number of different break sizes.

Figures 14A.6-1 and 14A.6-2 show the FLASH predictions of pressure versus time using the variable bubble velocity as compared with the measured data for the 100 percent break area and the 6.1 percent break area. Figure 14A.6-1 shows that, for the 100 percent break area, the FLASH code predicts depressurization to be complete in less than 2 sec as compared with 5 sec from the test data. This implies that the two-phase critical

0153

~~00005~~

flow rates employed in FLASH may be on the high side. Figure 14A.6-2 shows a good correlation of the test data for the 6.1 percent break area over the entire blowdown period.

Figure 14A.6-3 shows the comparison of the measured amount of residual water with the FLASH predictions using the variable bubble velocity model. FLASH runs for break sizes smaller than 6.1 percent areas have not been made. The curve shows that the predicted residual mass is less than the measured residual mass for leaks larger than 7 percent full opening. Also, the FLASH runs did not take into account the heat added to the water from the hot metal. This becomes significant especially for very small ruptures since the vessel has a longer time to dump its heat into the water. If this heat input were considered in FLASH, it would result in a smaller percentage of water remaining than those shown on Figure 14A.6-3

If a constant bubble velocity of 2 ft/sec were used instead of the variable, the FLASH program would predict that 2 percent of the mass remains for the 6.1 percent break area. As seen from Figure 14A.6-3, 22 percent of the initial mass remains 3 min after depressurization. Therefore, even though the variable bubble velocity underpredicts the amount of water remaining, it is better than the constant value of 2 ft/sec used in the original version of FLASH.

Regardless of which bubble velocity model is used, the amount of water remaining for large ruptures with no injection is very small. For smaller ruptures some differences do exist depending on the leak location.

3 | A typical example is shown in Figures 14A.6-4 and 14A.6-5. These figures show the reactor vessel water volume and pressure for the assumed rupture of the pressurizer surge line. Only the two low pressure injection pumps and one of the three high pressure injection pumps were used. No credit was taken for the core flooding tanks. Figure 14A.6-4 shows that the minimum water level in the core is 2 ft higher for the case where the variable bubble velocity model was used. This is due primarily to a slightly higher enthalpy and a corresponding lower density at the leak for the case of the varying bubble velocity. It is also due to the slightly lower pressure that exists at a given time for the variable velocity case towards the end of the blowdown. This causes the low pressure injection system to start injecting water at an earlier time and provides for a faster recovering of the core.

In the reactor the core flooding tanks would start injecting water at 135 to 140 sec in both cases. The minimum water level that is reached is less than a foot below the top of the core using the constant VBUB model and is never below the top of the core in the variable VBUB model. In either case, adequate core cooling is always provided.

0154 ~~00066~~

14A.6.3 Design - High Pressure Injection Equipment

| 2

The design of the high pressure injection equipment is not at all affected by the bubble velocity model that is used. This system is designed to accommodate breaks in the system up to 3 in. in diameter with one of the two high pressure injection pumps operating without uncovering the core. This is true regardless of the location of the leak, i.e., in the hot or cold leg. The bubble velocity model that is used in this analysis is relatively unimportant since the rate of depressurization is such that separation will occur with a bubble velocity of 2 ft/sec. Also, in the pressure range of interest for the design of the high pressure injection equipment, the variable bubble velocity only varies from 1.5 ft/sec at 2,200 psia to 3.3 ft/sec at 600 psia. The variable velocity model is therefore comparable with the constant velocity model for these leak sizes and over this pressure range.

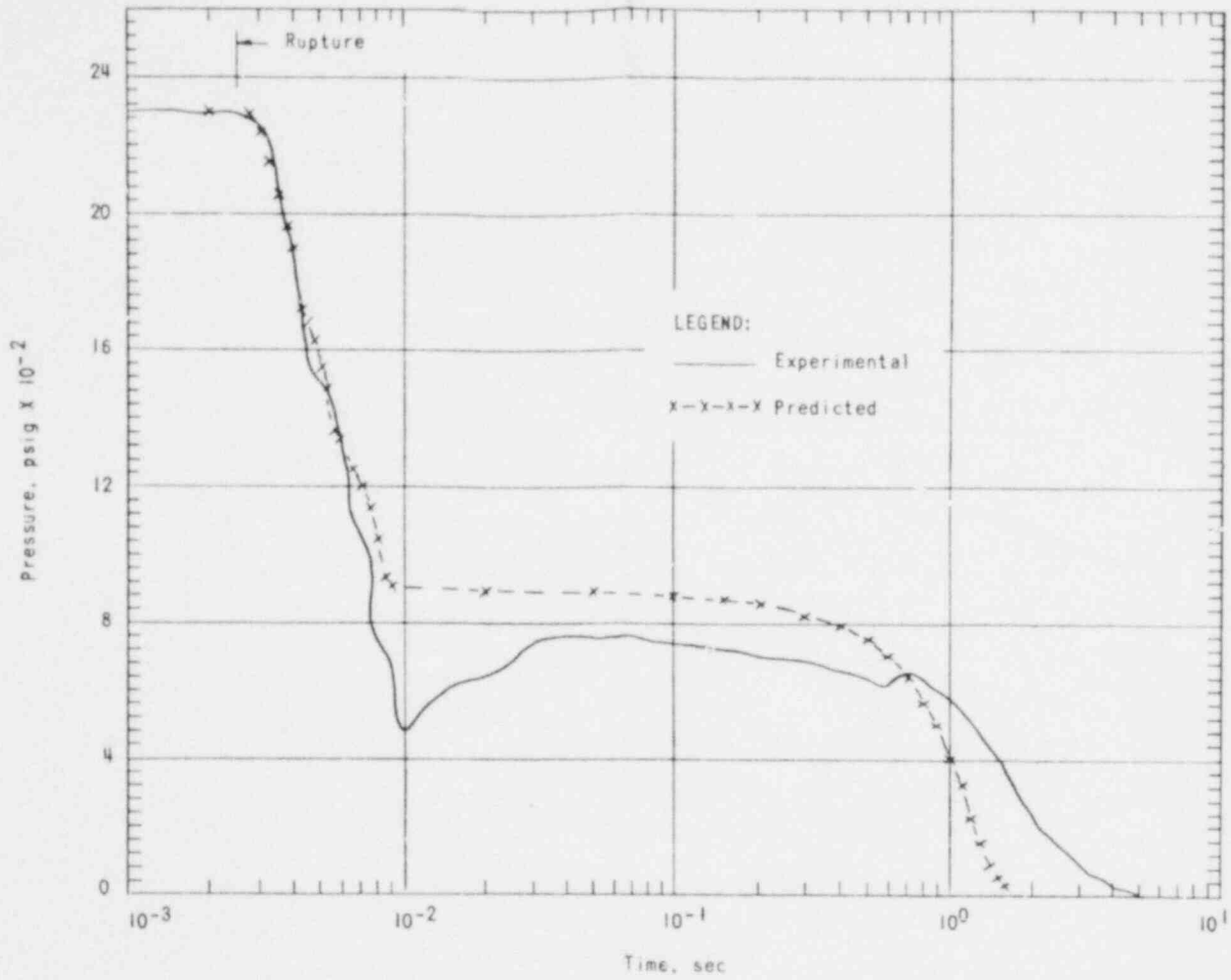
| 2

REFERENCE

<sup>1</sup>Wilson, J.F., et al, "The Velocity of Rising Steam in a Bubbling Two-Phase Mixture," Transactions of the ANS, Vol. 5, No. 1, p 151, June 1962.

~~00071~~

0155



~~00072~~

0156

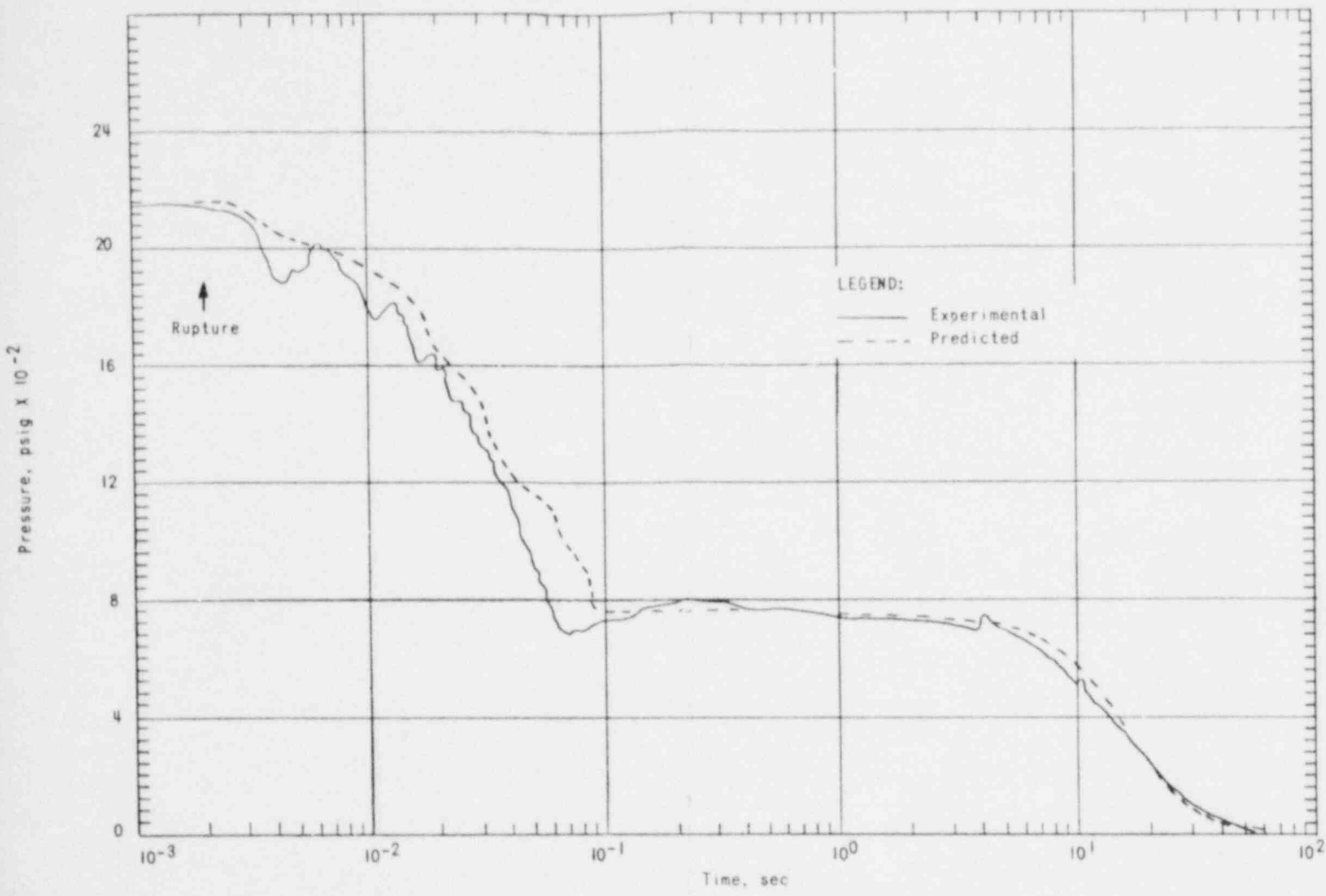
FIGURE 14A.6-1  
 VESSEL PRESSURE VERSUS TIME - 4-INCH  
 ID TOP RUPTURE. LOFT TEST NUMBER  
 548, 100 PERCENT BREAK AREA



**SMUD**

SACRAMENTO MUNICIPAL UTILITY DISTRICT

Amendment 1



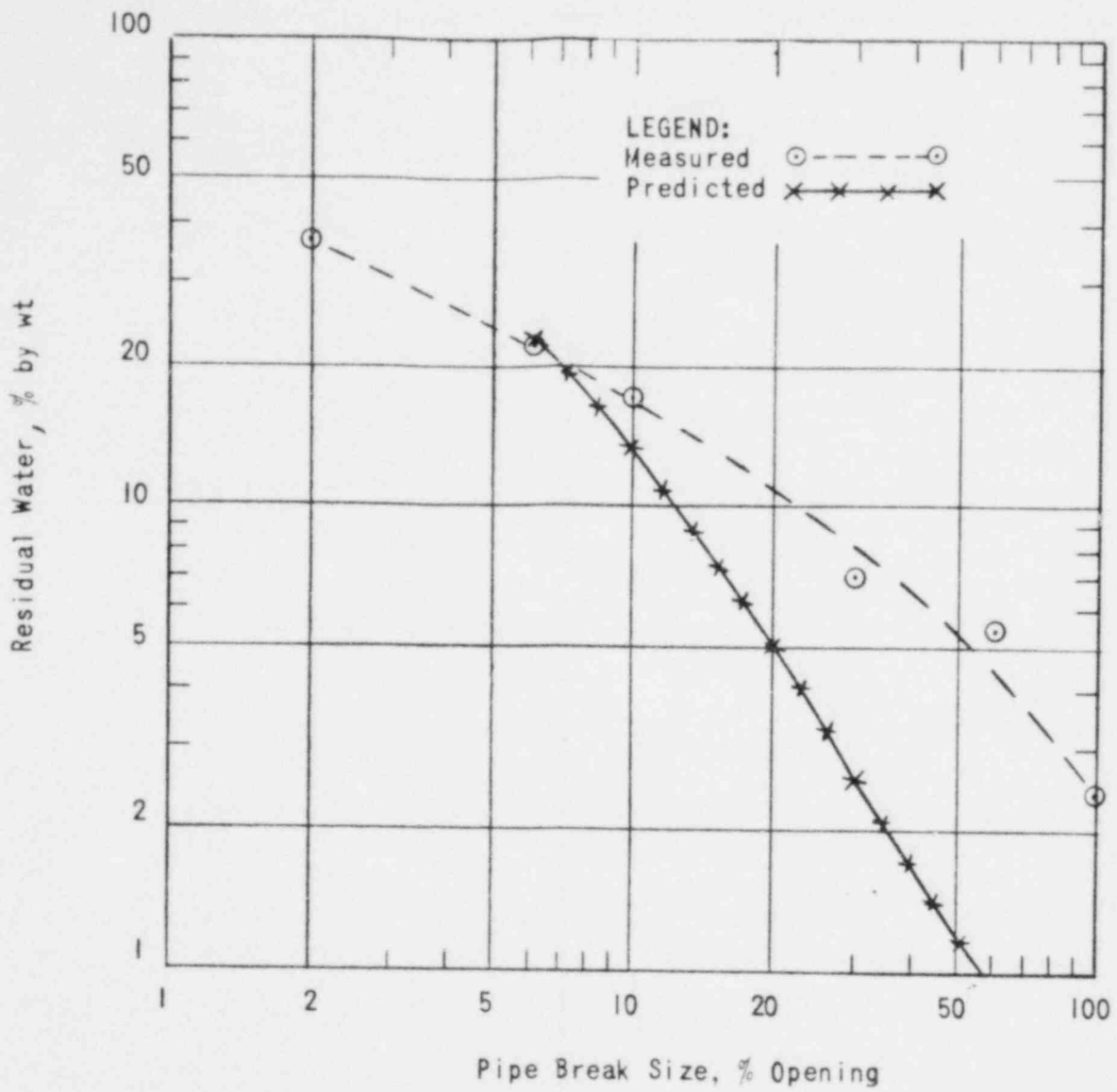
~~00073~~

FIGURE 14A.6-2  
 VESSEL PRESSURE VERSUS TIME - 6.1  
 PERCENT BREAK AREA LOFT SEMISCALE  
 BLOWDOWN TEST NUMBER 546

0157



Amendment 1



~~00074~~

FIGURE 14A.6-3  
 RESIDUAL WATER IN AN UNOBSTRUCTED  
 REACTOR VESSEL AFTER TOP BLOWDOWN  
 (520 F AND 2,330 PSIG)

0158



**SMUD**

SACRAMENTO MUNICIPAL UTILITY DISTRICT

Amendment 1

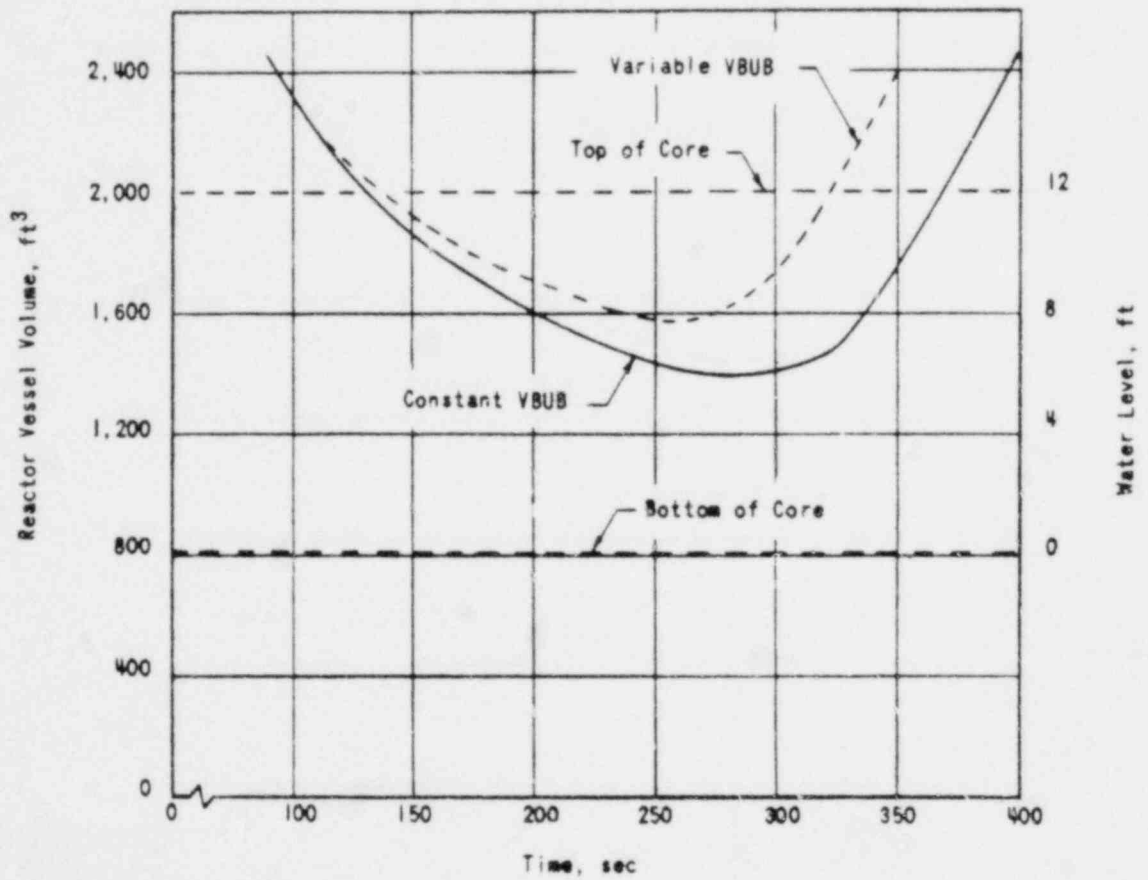


FIGURE 14A.6-4  
 REACTOR VESSEL WATER VOLUME VERSUS TIME  
 AFTER A SURGE LINE RUPTURE (0.4 FT<sup>2</sup>)  
 WITH OPERATION OF ONE HIGH PRESSURE  
 AND TWO LOW PRESSURE INJECTION PUMPS

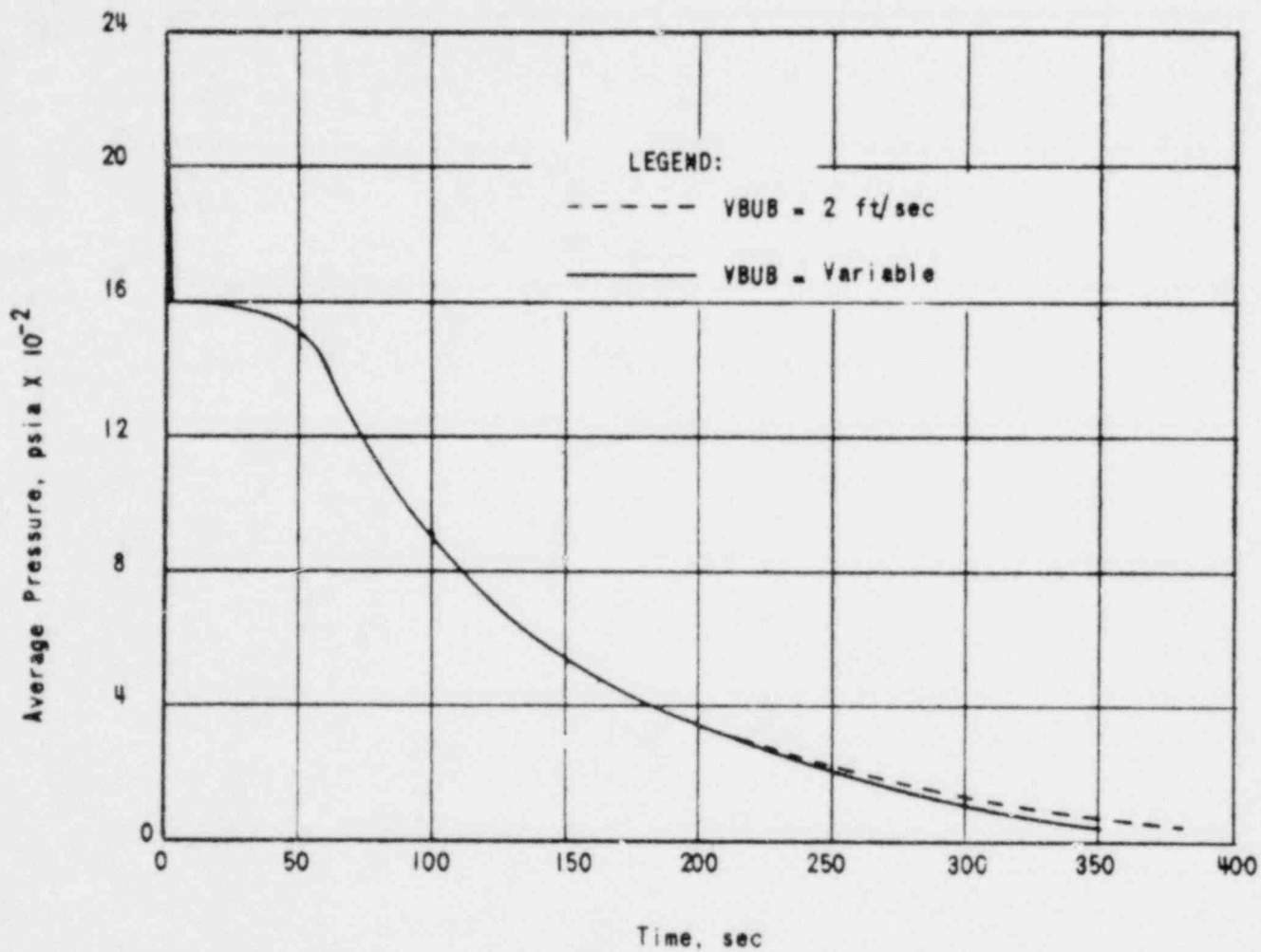
0159

~~00075~~



**SMUD**

SACRAMENTO MUNICIPAL UTILITY DISTRICT



~~00376~~

FIGURE 14A.6-5  
 REACTOR COOLANT AVERAGE PRESSURE VERSUS  
 TIME AFTER A SURGE LINE RUPTURE (0.4 FT<sup>2</sup>)  
 WITH OPERATION OF ONE HIGH PRESSURE  
 AND TWO LOW PRESSURE INJECTION PUMPS

0160



**SMUD**

SACRAMENTO MUNICIPAL UTILITY DISTRICT

12



QUESTION  
14A.7

Justify the assumption that the amount of diversion of injection water to the ruptured line during blowdown accident is not significant in the sizing of the accumulator volume. Include a description of the physical phenomena in the annulus including the mass and velocity of water and steam for various break sizes during the period which the accumulators inject water.

ANSWER  
Refer to  
14.2.2.3

Three possible mechanisms have been postulated by which the diversion of emergency injection water could bypass the core and affect the size of the core flooding tanks. These are: (a) a steam bubble in the core could prevent the coolant from entering the bottom of the core, (b) blowdown flow could have sufficient velocity to carry the injected water along with the blowdown steam, and (c) the high temperature reactor coolant could flash the incoming injection water.

#### Hot Leg Ruptures

The hot leg ruptures provide a path for the coolant escaping from the reactor vessel up through the core and out the rupture. The injection flow is down the thermal shield annulus to the bottom of the reactor vessel and then up through the core. Since the flow direction for all hot leg ruptures is up through the core and out the rupture, none of the above mechanisms can cause a bypass or diversion of the emergency injection water.

#### Cold Leg Ruptures

However, the large, cold leg ruptures have a leakage path which is down through the core and up the thermal shield to the rupture. The injection point is between the bottom of the core and the rupture; therefore, the above postulated mechanisms have been evaluated for these rupture locations.

##### a. Steam Bubble in the Core

The steam bubble could divert injection flow if the steam pressure in the core were adequate to depress the water level in the core and prevent injection from filling the core. The vent valves in the upper portion of the core support barrel provide for pressure equalization, which eliminates depression of the core water level and vents steam directly to the rupture. (These are discussed in detail in Appendix 3A.)

0161

b. Carryover

The second postulated bypass mechanism is that of the escaping coolant having sufficient velocity to carry over the injection water to the rupture. The point of contact of these two fluids is in the thermal shield annulus which has a flow area of approximately 33 ft<sup>2</sup>. For a piston effect to occur, a floating slug of cold, dense (56 lb/ft<sup>3</sup>), injection water on a flowing stream of steam (6.7 lb/ft<sup>3</sup>, average mixed density of escaping coolant at time injection starts) must exist. For the slug to sustain its position or move outward, the velocity must remain high enough to support the fluid piston, then pass around the cold water, and escape through the rupture.

At the time injection starts for the double-ended inlet pipe rupture, the flow rate in the core and thermal shield annulus is less than 4,000 lb/sec. Assuming this is all saturated steam at 600 psi, the velocity of the escaping fluid is approximately 84 ft/sec which would produce a stagnation pressure of 1.1 psi to hold up the fluid piston. This pressure is adequate to support a columnated slug of water approximately 2.8-ft high.

Two seconds later, at 10 seconds after the rupture, the flow is less than 1,000 lbs/sec, and the average density of escaping coolant is 0.65 lbs/ft<sup>3</sup>. The resultant velocity in the annulus is now reduced to 56 ft/sec which can produce a stagnation pressure of only about 6 in. of water. With this reduction in stagnation pressure a suspended fluid slug in the annulus must be collapsing and moving downward under the influence of gravity.

At 13 sec, or 5 sec after injection has started, the annulus flow is less than 500 lb/sec, and the density of the escaping coolant has decreased to 0.35 lb/ft<sup>3</sup>. The annulus velocity is only 37.4 ft/sec and can produce a stagnation pressure of only 1.5 in. of water. The water is again unrestrained against free fall.

Thus, it can be seen that the stagnation pressures developed by the steam flowing in the injection annulus cannot support a significant slug of injection water. For a short time the stagnation pressures could offer a small resistance to free fall, but this pressure rapidly decreases to the point that the injected fluid can fall freely under gravity.

0162

~~00078~~

c. Flashing

The third postulated mechanism is that of the escaping fluid flashing the incoming injection water. This has been evaluated by assuming a flashing model in which the injection flow rate and the escaping fluid become perfectly mixed. Using a 280 F as energy datum (point at which the condensing fluid would not flash at the end of blowdown), the escaping coolant could flash the incoming liquid for approximately the first 1.5 sec of injection. Beyond this time the injection flow can completely condense the escaping steam flow in the annulus. The injection up to this time is approximately 150 ft<sup>3</sup> and represents only 8 percent of the core flooding tank inventory. This loss of inventory in the reactor vessel would be more than compensated by the gain from complete condensation during the remaining 5.5 sec of the blowdown.

The reactor vessel annulus represents a large flow area available for the injection water, and only 10 to 25 percent of this flow area is required. Thus, no mechanism for intimate mixing is justified. Since the flowing reactor coolant will only offer a small resistance to injection coolant flow, and since the reactor coolant cannot flash a significant amount of the injection coolant, there is no way for a significant quantity of the injection coolant to be diverted to the leak.

A similar analysis has not been made for the complete spectrum of leak sizes as the double-ended pipe rupture requires the greatest amount of injection in the shortest period to time. In addition, the smaller break sizes will leave behind a greater percentage of the original reactor coolant, and therefore less injection coolant is required.

0163

~~00379~~

QUESTION 14A.8 Provide an analysis of local pressure forces imposed by primary coolant piping breaks within the primary cavity.

14A.8.1 What is the largest break which the primary cavity can withstand (the pressure transient and criterion for failure should be included).

14A.8.2 What is the largest break size possible within the cavity or shield, what piping restraints will be provided and what pressure transient and loading does this impose.

14A.8.3 Perform a similar analysis of local pressures resulting from a break outside the primary cavity.

ANSWER 14A.8

The pressure transient following a primary coolant system rupture within either the reactor cavity or the steam generator compartment is governed by the relative magnitudes of the flow rates associated with 1) the input of material into the volume from the rupture, and 2) the exit of material through openings in the boundaries of the compartment. The COPATTA computer program has been modified to include equations which describe the flow through these relief areas.

This new version of the code has been used to study the consequences of a coolant pipe rupture within either the steam generator compartment or the reactor cavity. A spectrum of break sizes was considered, with the relief area treated as a design parameter.

14A.8.1 In the case of the reactor cavity, it was found that an 8.5 ft<sup>2</sup> rupture can be accommodated with a relief area of approximately 125 ft<sup>2</sup> without compromise of the functional capability of the primary shield. This rupture size corresponds to a complete double ended severance of a cold leg primary coolant line.

14A.8.2 Restraints will be provided on the 36" I.D. hot leg coolant lines to insure that a rupture larger than 8.5 ft<sup>2</sup> is not possible.

14A.8.3 The results for the case of the steam generator compartment are shown in Figure 14A.8-1. The final design will include sufficient vent area to be compatible with the structural strength of the walls for the 14.1 ft<sup>2</sup> case.

2

0164

~~00000~~

SUPPLEMENTAL ANSWER TO QUESTION 14A.7

Effects of Postulated Injection Coolant Diversion Mechanisms on Core Water Volume and Clad Temperature

1. Introduction

In Section 14.2.2.3 of the Rancho Seco PSAR the analysis of cold leg piping ruptures has been presented on the basis that the injection water would be introduced into the water vessel without any loss due to diversion by carryover or flashing. The water level would rise in the core directly proportional to the amount of coolant injected (unrestricted flooding), and no credit was taken for condensation effects to increase the water inventory. Core cooling was not assumed after blowdown was completed until the water level reached the hot spot elevation. The maximum clad temperature experienced during a 28 inch ID double-ended cold leg pipe rupture was 1785 F.

In Question 14A.7 of Amendment I, a discussion was presented that discussed the potential mechanisms of the diversion of the injection water and their effect upon the cold leg loss of coolant accident. Large cold leg ruptures have two leakage paths in the reactor vessel; (1) through the vent valves to the vessel downcomer annulus, and (2) through the core, up the vessel downcomer annulus between the vessel wall and the thermal shield to the rupture. Since the injection water enters the reactor vessel in this annulus, the postulated mechanisms for diverting injection coolant were: (1) diversion by carryover of the injection water by escaping steam, and/or flashing of the injected coolant, and (2) a steam bubble in the core. This analysis showed that the net effect of diversion of injection coolant on water inventory would be insignificant. In response to informal questions regarding our analysis of the effects of injection water diversion, a supplemental analysis is supplied.

In the evaluation of these postulated mechanisms, the criterion of acceptance is the effect of injection diversion upon peak clad temperatures. The core flooding system design criterion is to limit the hot spot clad temperature to 2300 F as stated in Section 14.2.2.3 of the PSAR.

2. Effects of Injection Diversion

The water level in the core as a function of time as presented in Figure 14.2-32 of the PSAR conservatively assumed that the inventory was a function of injection rate only and did not include any effects of water remaining, condensation, or carryover. The rate of coolant rise into the core is unrestricted by the pressure buildup in the reactor vessel upper plenum. This analysis is conservative because:

0165

~~00081~~

- a. If the water remains in the system to form the water seal in the cold leg piping, water must also remain in the reactor vessel and fill times will be shorter. If primary water does not remain, unrestricted flow into the core will be approached.
- b. The diversion of injection water will be more than compensated for by condensation effects.

In order for the injection water to be diverted out the leak due to carryover by the steam, the water will have to intimately mix with the steam. The annulus geometry is such that intimate mixing will be difficult to obtain and the water injected should go directly to the bottom of the vessel. Water from the core flooding tanks enters the reactor vessel through two nozzles 180° apart. The centerlines of the flooding nozzles and the main reactor coolant pipe nozzles are 30° apart (~ 3.6 ft) at the closest point. The injection nozzles enter the vessel at an elevation just above the main coolant nozzles and just below the vent valves. The flow deflectors on the core support shield and the vent valve steam flow forces will tend to direct the injection flow toward the bottom of the vessel.

While the geometry makes it very unlikely that injection coolant would be lost by diversion to the leak, it cannot be proved conclusively. Accordingly, an analysis has been made assuming that mixing of the leak flow mixture and the injection water does occur. For the first two seconds of injection, the period from 7.5 to 9.5 seconds after the rupture, the energy content of the steam flowing out the leak is greater than the heat absorption capability of the injected coolant. After the first 2 seconds of injection, all of the leakage steam flow can be condensed by the injection water and cooled down to the saturated condition at 65 psia.

Relating this to volume and assuming that diversion will occur if all of the steam cannot be condensed, 150 ft<sup>3</sup> of injection water could be lost during the first 2 seconds of injection. However, condensation and cooling that occurs during the remainder of the blowdown results in a gain of slightly more than 150 ft<sup>3</sup>. Assuming that no water remains in the steam generators and the reactor coolant inlet lines to form a water seal, the unrestricted fill curve of core water level versus time shown on Figure 14.2-32 of the PSAR also applies to the accident condition in which injection coolant is diverted until it can condense the leaking steam flow. This essentially identical fill rate curve will yield the same peak hot spot temperature of 1785 F. To demonstrate the sensitivity of core water height to diversion effects, Figure 14A.7-1 shows both the unrestricted fill rate curve and a curve obtained by assuming that diversion of all injection water occurs for the first 4 seconds (twice the time period that is physically possible based upon heat balance considerations). No credit is taken for any condensation or water

0166

~~00082~~

remaining and this results in a loss of 380 ft<sup>3</sup> of injection water. The net effect of this latter case is to shift the water level versus time curve approximately 4 seconds and delay core cooling. This increases the peak hot spot temperature to 1960 F.

One of the LOFT semiscale blowdown tests was made with an internals configuration which roughly simulated the internals configuration of a large PWR with vent valves in the core support barrel. Preliminary results from this test indicate that as much as 20% of the water could be left in the reactor vessel if a vent is available for the steam. Such a vent is available in the Rancho Seco reactor vessel internals. Recognizing that differences exist between this test and the reactor, a curve has been generated which assumes that only 1/2 of the test results or 10% of the vessel inventory remains at the end of blowdown. This curve, also shown on Figure 14A.7-1, assumes that 10% (≈ 400 ft<sup>3</sup>) of the reactor vessel water volume remains in the vessel and includes 2 seconds of injection water diversion with the compensating effects of condensation. The net effect of this case is to shift the water level versus time curve back in time approximately 4 seconds and to reduce the peak hot spot clad temperature to 1600 F.

This analysis shows that the peak clad temperature is not extremely sensitive to the effects of water remaining or diversion of injection coolant. Even taking the extreme case of 4 seconds of diversion, no water remaining at the end of blowdown, and no condensation only increased the peak hot spot temperature from 1785 F to 1960 F which is still significantly below the design criterion value of 2300 F.

### 3. Effects of Core Support Shield Vent Valves

If a sufficient quantity of water were left in the steam generators following the blowdown and the vent valves were not incorporated into the design, the steam formed in the core could build the pressure up to the point where core filling could be delayed or prevented. However, the vent valves in the core support shield will open to equalize the pressure between the core outlet plenum and the downcomer annulus. The core cooling has been analyzed utilizing the characteristics of these vent valves. This analysis also assumed for the base case that no diversion or condensation occurred and that no water remained at the end of blowdown. The effect of these factors is included as a sensitivity analysis in this study.

Figure 14A-7.2 shows the water height as a function of time after a double-ended inlet pipe rupture for the case where a water seal exists in the inlet piping. The steam flow through the vent valves provides for pressure equalization but the core flooding rate is restricted by the pressure buildup in the reactor vessel upper plenum. This curve is based upon the

0107

~~00003~~

quiet water level and no credit is taken for increased elevation due to the existence of a steam-water mixture. The curve of fill rate for the unrestricted condition is shown for comparison purposes.

The time to cover the hot spot is delayed only 3 seconds if a water seal exists. While the water level as a function of time in the lower region of the core is affected only slightly, the upper region of the core is uncovered for a longer period of time. This is due to the high steam generation rates that exist during this phase of the accident. With these longer filling times, the temperature conditions for the hot spot, core midpoint and 3/4 point have been calculated based on steam cooling after the quiet water level enters the core and generates significant quantities of steam. Figure 14A-7.3 shows that when the water reaches the hot spot (the 1/4 point) at 23 seconds, the steam generation rate is 180 lb/sec. This steam generation rate provides a steam cooling heat transfer coefficient of  $\approx 20$  Btu/hr-ft<sup>2</sup>-°F. From the time water enters the core at 16 seconds until the hot spot is covered, the heat transfer coefficient at the hot spot increases from 0 to 20 as a function of steam flow.

The hot spot cladding temperatures are shown on Figure 14A-7.4. The case using restricted flow includes steam cooling and yields a peak temperature of 1760 F. The unrestricted flow case as reported in the PSAR does not utilize any cooling until the water reaches the quarter point and a peak temperature of 1785 F results. Figures 14A-7.5 and 14A-7.6 show the hot channel clad temperatures at the midpoint and 3/4 point elevations in the core based on steam cooling. From Figure 14A-7.2, it can be seen that the midpoint and 3/4 point elevations are covered at 54 seconds and 105 seconds, respectively. The maximum temperature for the midpoint is 1615 F and the maximum temperature for the 3/4 point is 1430 F. The temperatures at both of these points are lower than the peak temperature of 1760 F at the core hot spot. This analysis demonstrates that the vent valves are adequate to assure core cooling in the event of a large cold leg rupture.

Again, to demonstrate the effects of diversion, condensation, and the water remaining, on the core flooding rates, this analysis has been extended using the same injection assumptions as for the unrestricted flooding cases. The core water level as a function of time after rupture is shown on Figure 14A-7.7. The three curves on this figure represent four different injection conditions: (1) the base case which represents the level as a function of injection only with no diversion, condensation or water remaining, (2) the 2 second diversion case with condensation which results in an identical curve as the base case, (3) the 4 second diversion case without condensation, and (4) the 10% water remaining case with 2 seconds of diversion with condensation.

The base case condition as well as the identical fill rate case resulting from 2 seconds of diversion and condensation yields a peak hot spot

0168

~~00084~~



temperature of 1760 F. The extreme case of assuming diversion for twice the time possible from heat balance considerations, and neglecting condensation effects results in a peak temperature of only 1935 F. This is considerably lower than the design criteria value of 2300 F. The 10% water remaining case lowers the peak temperature to 1575 F.

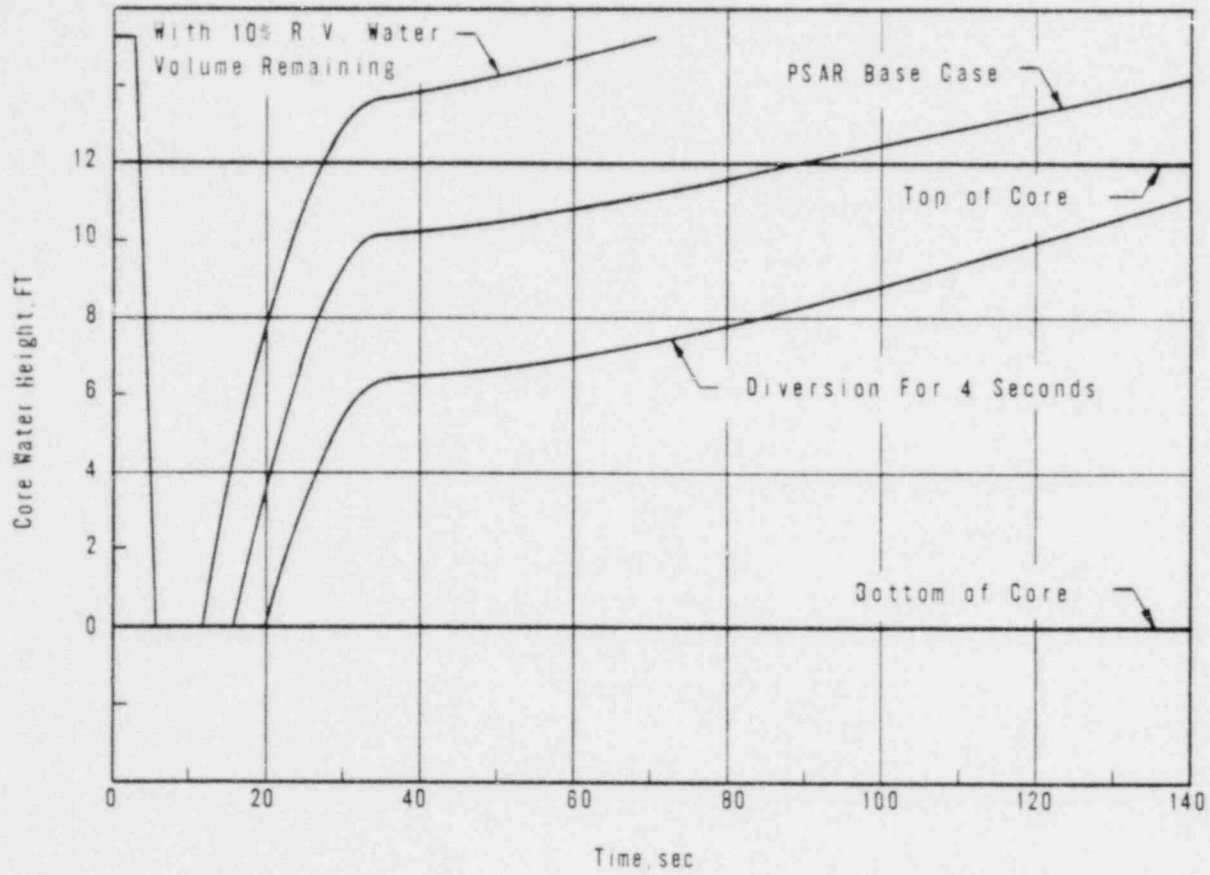
#### 4. Conclusions

The analysis presented above included the effects of (a) injection coolant diversion, with and without compensating condensation effects, (b) water remaining in the reactor vessel, and (c) the two modes of venting the steam generated in the core during reflooding. This analysis demonstrates:

- a. That diversion effects, if they occur, will be compensated for by condensation effects and the peak hot spot temperatures will be approximately the same as for the case that assumed no diversion or condensation.
- b. That water remaining in the reactor vessel provides a beneficial effect of lower peak clad temperatures. This effect is not included in the design basis analyses although experimental data indicates that water will remain. Thus, it represents a conservative factor in the analysis.
- c. That the peak clad temperature is relatively insensitive to diversion, condensation, and water remaining. Even the extreme diversion case (4 sec diversion) representing a loss of 20% of the CFT inventory only increased the peak hot spot clad temperature to 1960 F which is well below the design criteria value of 2300 F and only 175 F higher than the base case value.
- d. That the difference between the peak temperatures both for the unrestricted steam venting condition and for steam venting with just the core support shield vent valves is small. Therefore, the vent valves are adequate to provide the necessary core cooling.

0169

~~00795~~



~~00006~~

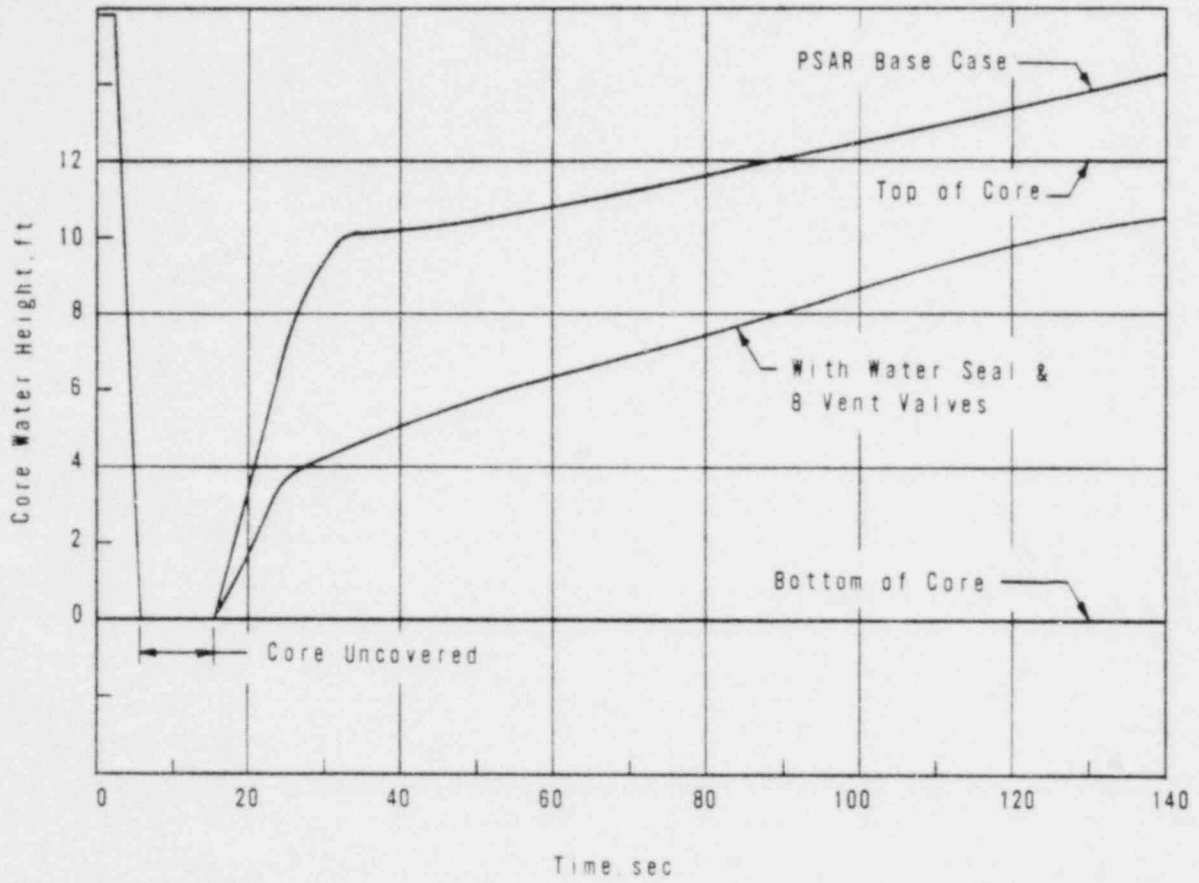
0170

FIGURE 14A.7-1  
 UNRESTRICTED FILL-CORE QUIET  
 WATER HEIGHT FOR A 28-INCH ID,  
 DOUBLE-ENDED, COLD-LEG PIPE RUPTURE



**SMUD**

SACRAMENTO MUNICIPAL UTILITY DISTRICT



~~00307~~

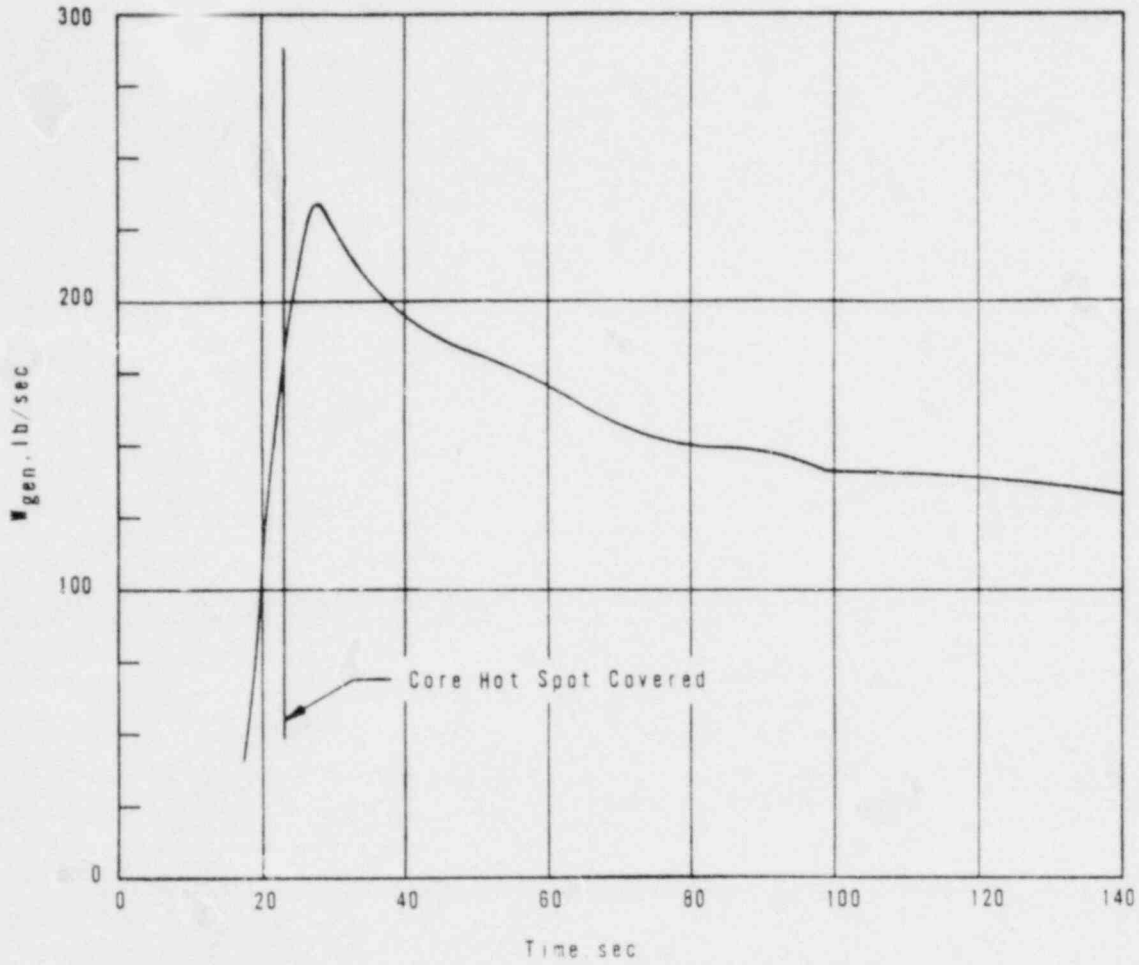
0171

FIGURE 14A.7-2  
CORE QUIET WATER HEIGHT FOR  
A 28-INCH ID, DOUBLE-ENDED,  
COLD-LEG PIPE RUPTURE



**SMUD**

SACRAMENTO MUNICIPAL UTILITY DISTRICT



~~00000~~

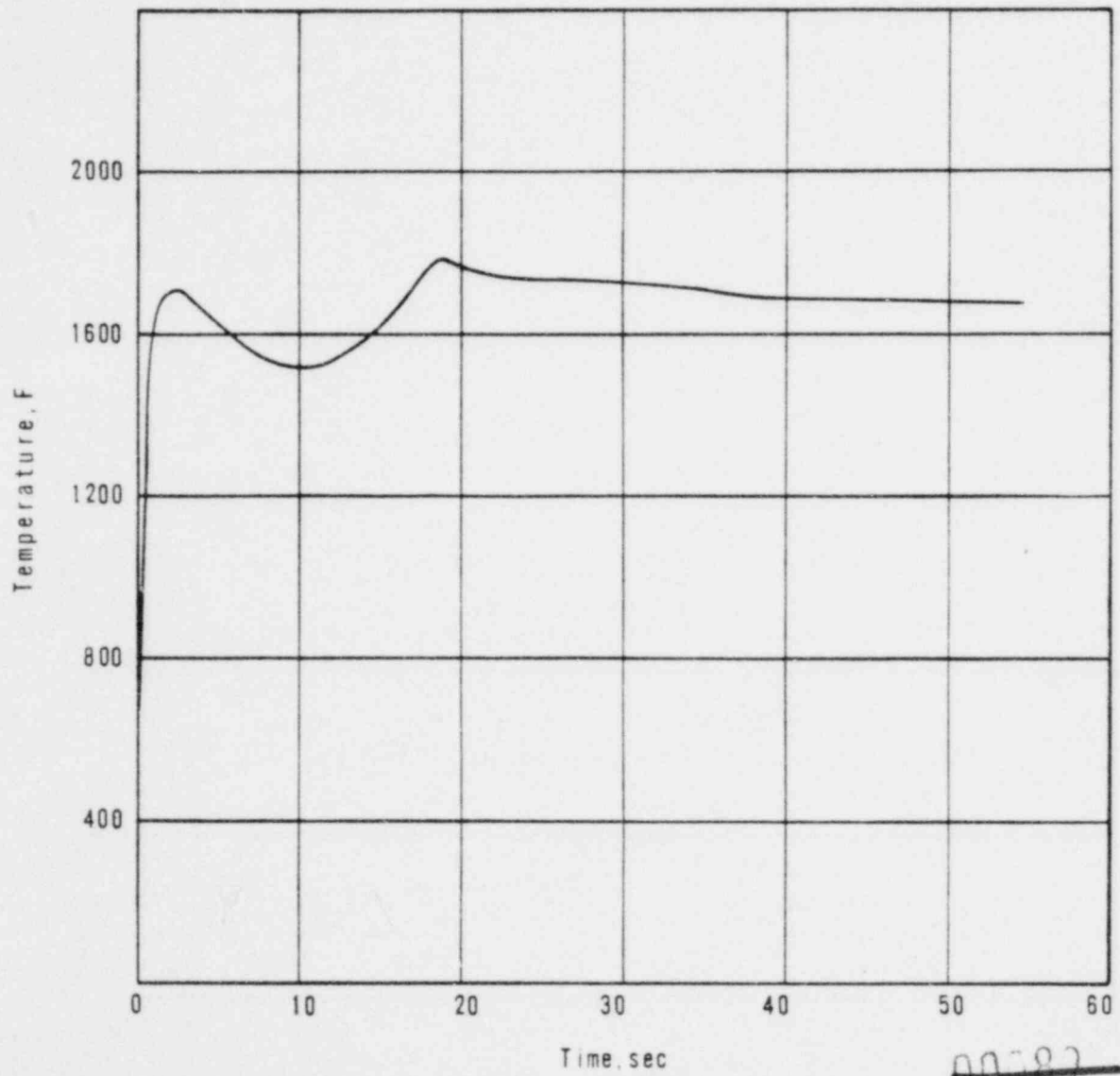
0172

FIGURE 14A.7-3  
 CORE STEAM GENERATION RATE DURING  
 REFILL FOR A 28-INCH ID, DOUBLE-ENDED,  
 COLD-LEG PIPE RUPTURES, BASE CASE



SACRAMENTO MUNICIPAL UTILITY DISTRICT

Amendment 4



~~00587~~

0173

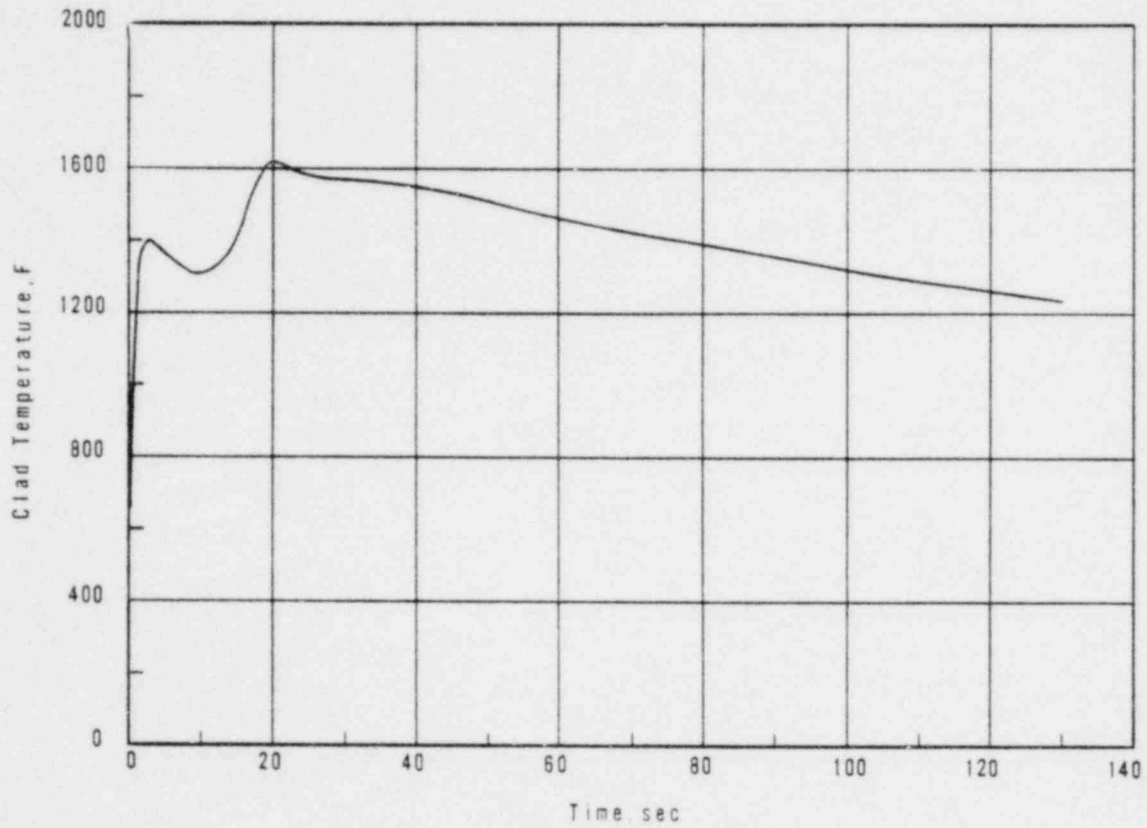
FIGURE 14A.7-4  
 CLAD HOT SPOT TEMPERATURE  
 FOR A 28-INCH ID, DOUBLE-ENDED,  
 COLD-LEG PIPE RUPTURE



**SMUD**

SACRAMENTO MUNICIPAL UTILITY DISTRICT

Amendment 4

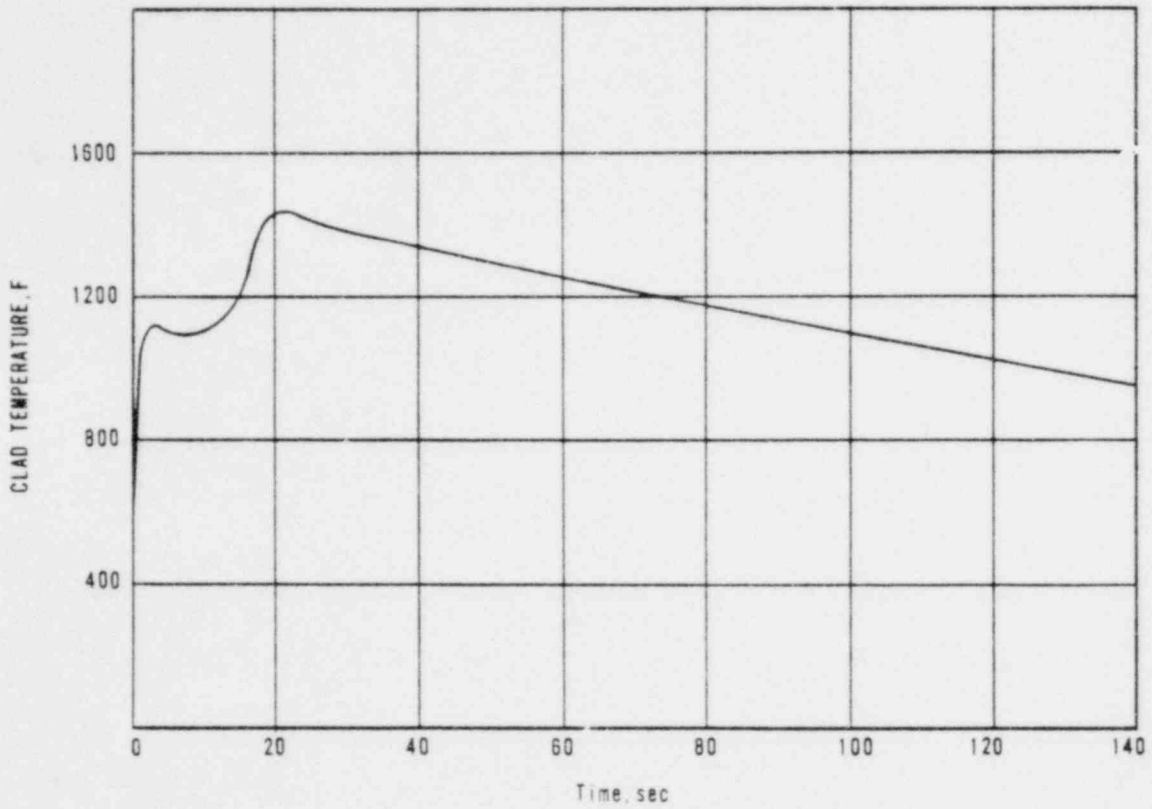


~~00090~~

0174

FIGURE 14A.7-5  
 CLAD TEMPERATURE AT CORE MIDPOINT  
 FOR A 28-INCH ID, DOUBLE-ENDED,  
 COLD-LEG PIPE RUPTURE





~~00391~~

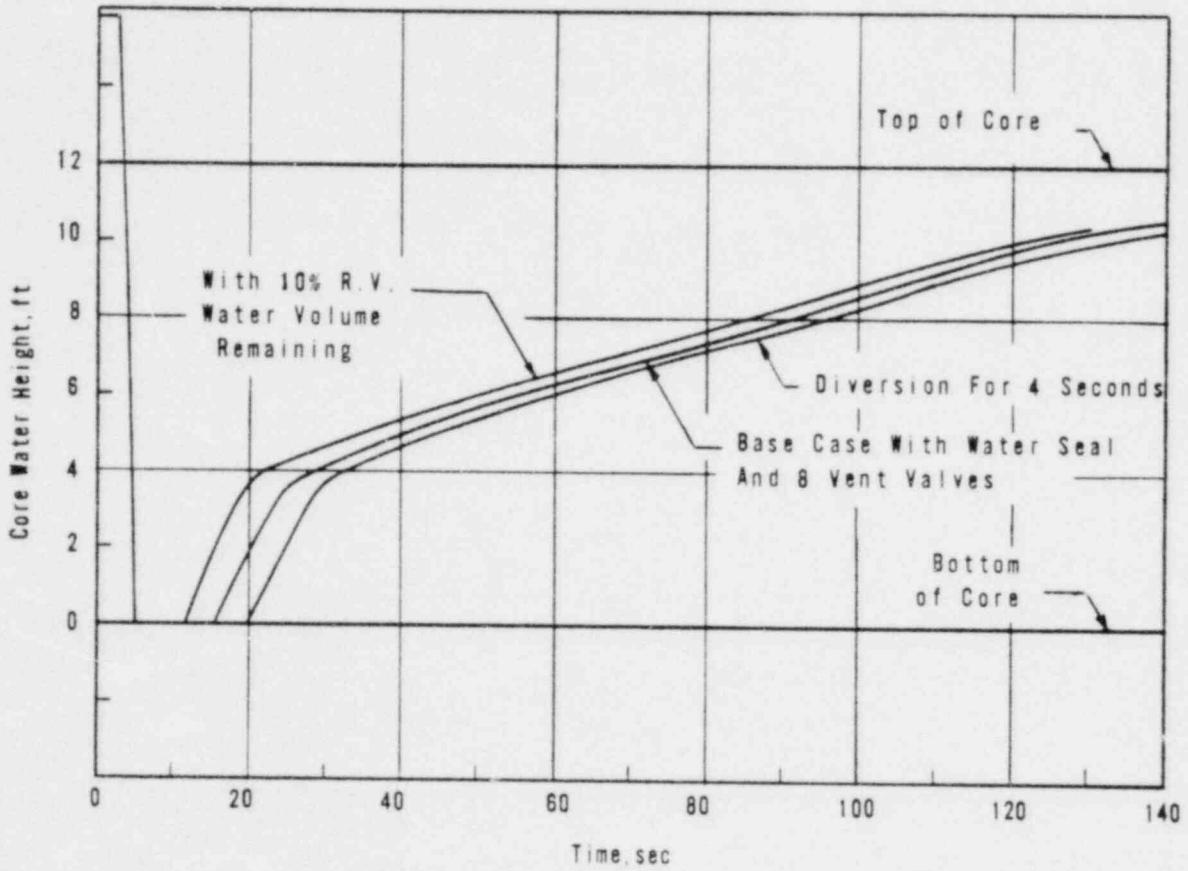
0175

FIGURE 14A.7-6  
 CLAD TEMPERATURE AT CORE 3/4 POINT  
 FOR A 28-INCH ID, DOUBLE-ENDED,  
 COLD-LEG PIPE RUPTURE



**SMUD**

SACRAMENTO MUNICIPAL UTILITY DISTRICT



~~00092~~

0176

FIGURE 14A.7-7  
 SENSITIVE ANALYSIS ON CORE QUIET  
 WATER HEIGHT FOR A 28-INCH ID, DOUBLE-  
 ENDED, COLD-LEG PIPE RUPTURE



**SMUD**

SACRAMENTO MUNICIPAL UTILITY DISTRICT



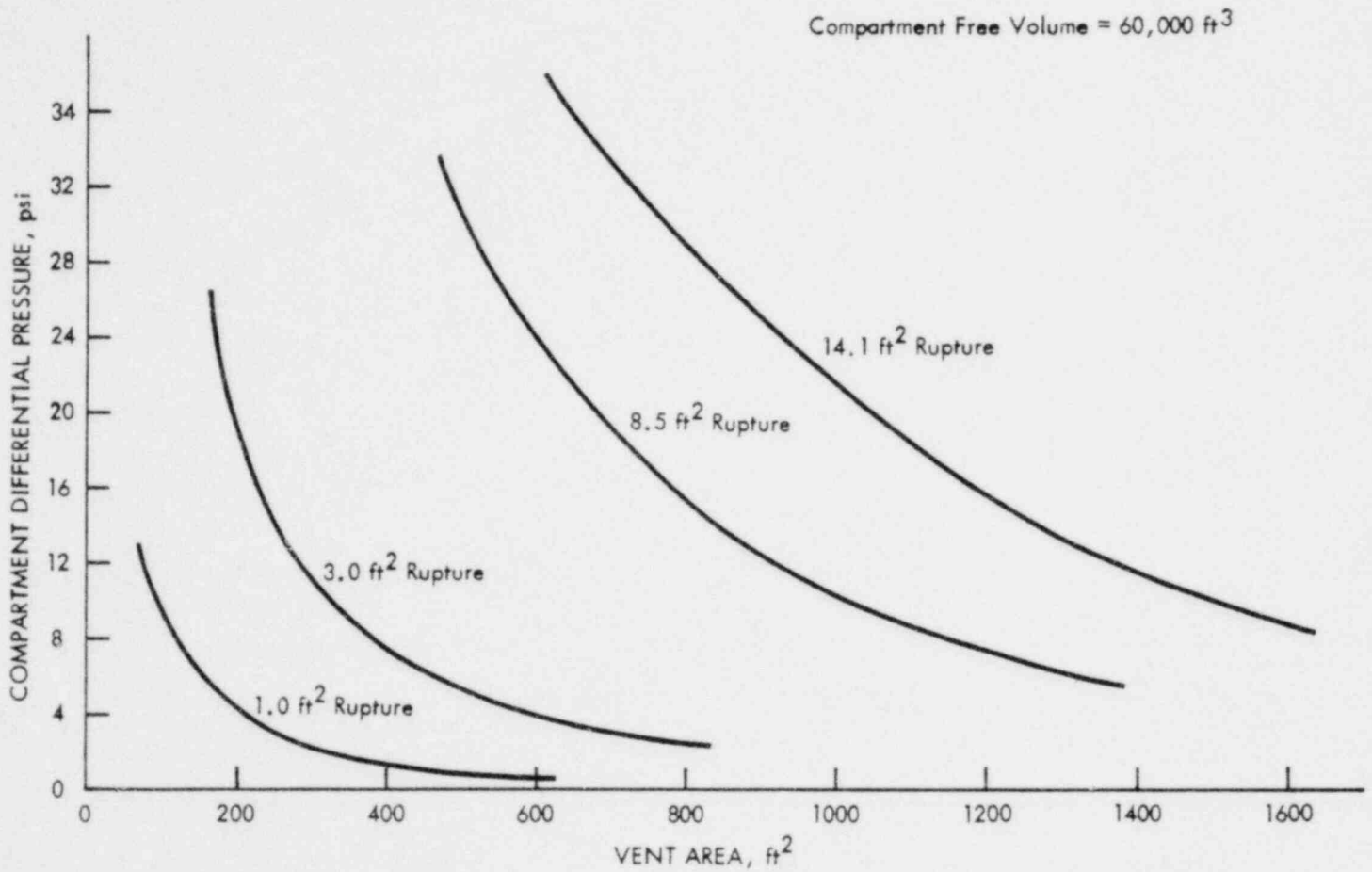


FIGURE 14A.8-1  
 STEAM GENERATOR COMPARTMENT  
 DIFFERENTIAL PRESSURE  
 FOLLOWING PIPE RUPTURE

0177

~~00093~~



**SMUD**

SACRAMENTO MUNICIPAL UTILITY DISTRICT

QUESTION  
14A.9

Discuss how the design basis accident releases and other accidental releases relate to the radiation monitoring system design including range, sensitivity and detector location.

ANSWER  
Refer to  
11.2.2

The answer to question 11A.1 discusses the radiation monitoring system and outlines the number, type and range of all radiation monitors. All monitors will be designed to have sufficient sensitivity to detect expected radiation levels.

The total curies released into the reactor building following the design basis accident is estimated to be  $17 \times 10^6$  curies, corresponding to the release of the total gap activity. If credit is taken for 95% removal of iodine by containment spray, the equivalent  $I^{131}$  concentration at the site boundary during the two-hour period following the accident is approximately  $1 \times 10^{-7}$  uc/cc. The  $Xe^{133}$  concentration is expected to be  $1.5 \times 10^{-5}$  uc/cc. For particulates, the  $Cs^{137}$  released during the accident will be available for leakage from the reactor building. All site monitors would give indication of the radiation levels at the site boundary following the design basis accident.

In addition to the design basis accident, the effects of other accidents, discussed in Section 14 of the PSAR, upon the radiation monitoring system have been investigated. These include steam generator tube leakage, steam line failure, loss of electric power, rod ejection accident, and a fuel handling accident.

For the rod ejection accident it is assumed that the resulting power excursion damages fuel rods, releasing 166,000 curies of  $I^{131}$  and  $1.45 \times 10^6$  curies of noble gases to the containment building. Assuming that the containment building leakage is 0.1 percent of the containment volume per day, and assuming 95% removal of iodine by containment spray, the  $I^{131}$  concentration at the site boundary following the rod ejection is about  $1.4 \times 10^{-8}$  uc/cc.

Considering the relationship of components of the environmental monitoring system to steam generator tube failure, 52,600 curies of noble gases are assumed to be released into the secondary water and through the condenser vents into the atmosphere. The resulting whole-body dose from this accident at the site boundary is calculated to be 0.77 rem, with a noble gas concentration of approximately  $1.2 \times 10^{-3}$  uc/cc for the two-hour period following the accident. The thyroid dose is 0.007 rem at the site boundary, and the corresponding  $I^{131}$  concentration is about  $1.2 \times 10^{-9}$  uc/cc. The analysis of the loss of electric power assumes concurrent steam generator tube leakage and a two-minute period of steam relief, resulting in a short-term whole body dose of 0.015 rem at the site boundary.

For the steam line failure outside the containment building, again assuming steam generator tube leakage, an instantaneous, uncontained release of 224 curies of noble gases and 4.22 curies of equivalent I<sup>131</sup> is postulated. The integrated short-term exposure at the site boundary would be .003 rem to the whole body and a .306 rem thyroid dose. Estimated concentrations at the site boundary are  $3.2 \times 10^{-2}$  uc/cc and  $6 \times 10^{-4}$  uc/cc for noble gases and equivalent I<sup>131</sup>, respectively.

Relating the fuel handling accident to the atmospheric monitor in the plant vent, it is assumed that  $2.79 \times 10^4$  curies of noble gases and 28.4 curies of I<sup>131</sup> are released through the plant stack. If this occurs, the concentrations expected inside the plant vent are approximately  $2.8 \times 10^{-3}$  uc/cc I<sup>131</sup> and 2.74 uc/cc noble gases. If credit is taken for removal of 90% of the iodine by the high efficiency and charcoal filters, the I<sup>131</sup> concentration would be approximately  $2.8 \times 10^{-4}$  uc/cc. The monitor in the plant vent would record and alarm these values.

~~00095~~

0179

QUESTION  
14A. 10

Discuss the consequences to containment integrity and doses to the public if the design basis loss-of-coolant accident were to occur after the plant had been operating with steam generator tube leakage (at least 10 gpm) and secondary safety valve leakage. Discuss the implications of the calculation with respect to technical specification limits on operation of the plant with generator tube leakage and secondary safety valve leakage.

ANSWER  
Refer to  
14.3.8

The consequences to the public of simultaneous safety valve leakage of 10,000 lbs/hr, steam generator tube leakage of 10 gpm, and loss-of-coolant accident have been analyzed. This series of events could result in leakage from the reactor building, through the primary system, through the leaking steam generator tube, and then through the safety valve to the atmosphere. Leakage from the reactor building to the atmosphere via the leaking safety valve cannot occur until the pressure within the steam generator decreases to reactor building pressure. For a steam generator which contains 20,000 lbs of water, the minimum water inventory, blowdown to reactor building pressure requires 3.6 hours. Thus, the 2-hour doses at the exclusion distance are unchanged from the values reported in Section 14.2.2.3 of the PSAR.

After blowdown of the steam generator to reactor building pressure the pressure differential no longer prevents leakage. The leak rate from this path would result in an increase in the 30-day dose. If the containment building leakage rate of 0.1 percent per day is assumed, such a leakage rate would correspond approximately to 79 ft<sup>3</sup>/hr of containment atmosphere released to the environs. However, an additional leakage of 10 gpm through the leaking secondary system valve corresponds to approximately 80 ft<sup>3</sup>/hr. Consequently, it may be conservatively assumed that a 10 gpm leakage through the valve would about double the 30-day dose at the low population center from 0.026 rem to 0.052 rem. It is evident that even with a much higher leakage rate, doses at the low population center would meet 10 CFR 100 guide lines.

If no credit for iodine spray removal is taken then the dose at the site boundary would increase by a factor of approximately 20, from 0.026 to 0.52 rem in 30 days. Even under these assumptions a significantly higher than 10 gpm secondary valve leakage could be tolerated from the standpoint of doses at the low population center. However, the plant would not operate with a high leakage in the secondary system.

When the technical specifications are prepared, due regard will be given to plant operating limits imposed by potential steam

0180

generator tube and secondary safety valve leakage. When operational limits on steam generator tube leakage are prepared, the effects of leakage on secondary system water chemistry, primary system makeup rate, and boiler blowdown rate must also be considered. Similarly, when secondary system safety valve leakage limits are prepared, secondary system makeup and heat loss must be considered.

~~00097~~

0181

QUESTION  
14A.11

Provide calculations of the environmental effects resulting from an accident which released TID-14844 fission product fractions to the containment but in which 5% of the core iodine inventory is considered to be methyl iodide and that it is all released to the containment atmosphere (that is, 20% of the iodine in the containment atmosphere is in a nonremovable form). Also, a volumetric rather than a virtual source should be used for the release with a shape factor of one-half. Calculate the doses with and without thiosulfate spray.

ANSWER  
Refer to  
14.3.9

Figure 14A.11-1 presents doses to the thyroid as a function of the iodine fraction left in the containment air after sprays,  $F_s$ , and the containment leakage rate,  $\lambda_L$ . The iodine time removal constant,  $F_s$ , is assumed to be  $25.3 \text{ Hr}^{-1}$ , as discussed in section 14.3.10 of the PSAR.

It may be observed from this figure that if 20% of iodine remain airborne after thiosulfate sprays (corresponding  $F_s = 0.2$ ) and is available for leakage then the thyroid dose at the site boundary will be 41, 100, and 200 rem if the containment building leakage is 0.1, 0.25, and 0.5% volumes per day, respectively. It can be also observed that if only 50% of airborne iodine is removed (corresponding to  $F = 0.5$ ) then the building leakage rates of 0.1% ( $\lambda_L = 0.001$ ) and 0.25% ( $\lambda_L = 0.0025$ ) will not result in doses in excess of the AEC guideline values. If no airborne iodine is removed from containment atmosphere, the dose to the thyroid at the site boundary would be 170 rem with a 0.1% leakage rate and 430 rem with a 0.25% leakage rate.

Figure 14A.11-2 compares dilution factors for long-term releases at the Rancho Seco site. The solid line represents the dilution factor using the virtual point source distance to account for initial dilution in the "wake" of the containment building. The dashed curve shows the dilution factor using a volumetric rather than virtual point source. It may be observed that the volumetric source assumption provides a fractionally better dilution at the site boundary than the virtual front source assumption does.

0182

~~00090~~

QUESTION 14A.12 Discuss the effect of assuming heat transfer to the steam generator during blowdown on (1) the peak containment pressure, and (2) the core thermal transient.

ANSWER Peak Containment Pressure

Refer to 14.2.2.3 An analysis to determine the amount of heat transferred in the steam generator during the loss-of-coolant accident has been made for the 3.0 ft<sup>2</sup> hot leg rupture. This rupture produces the peak reactor building pressure.

There are three areas of interest:

- a. Heat transfer to steam generator during early blowdown.
- b. Heat transfer to the reactor coolant from the steam generator during the latter part of the blowdown.
- c. Heat transferred after depressurization of the reactor coolant system.

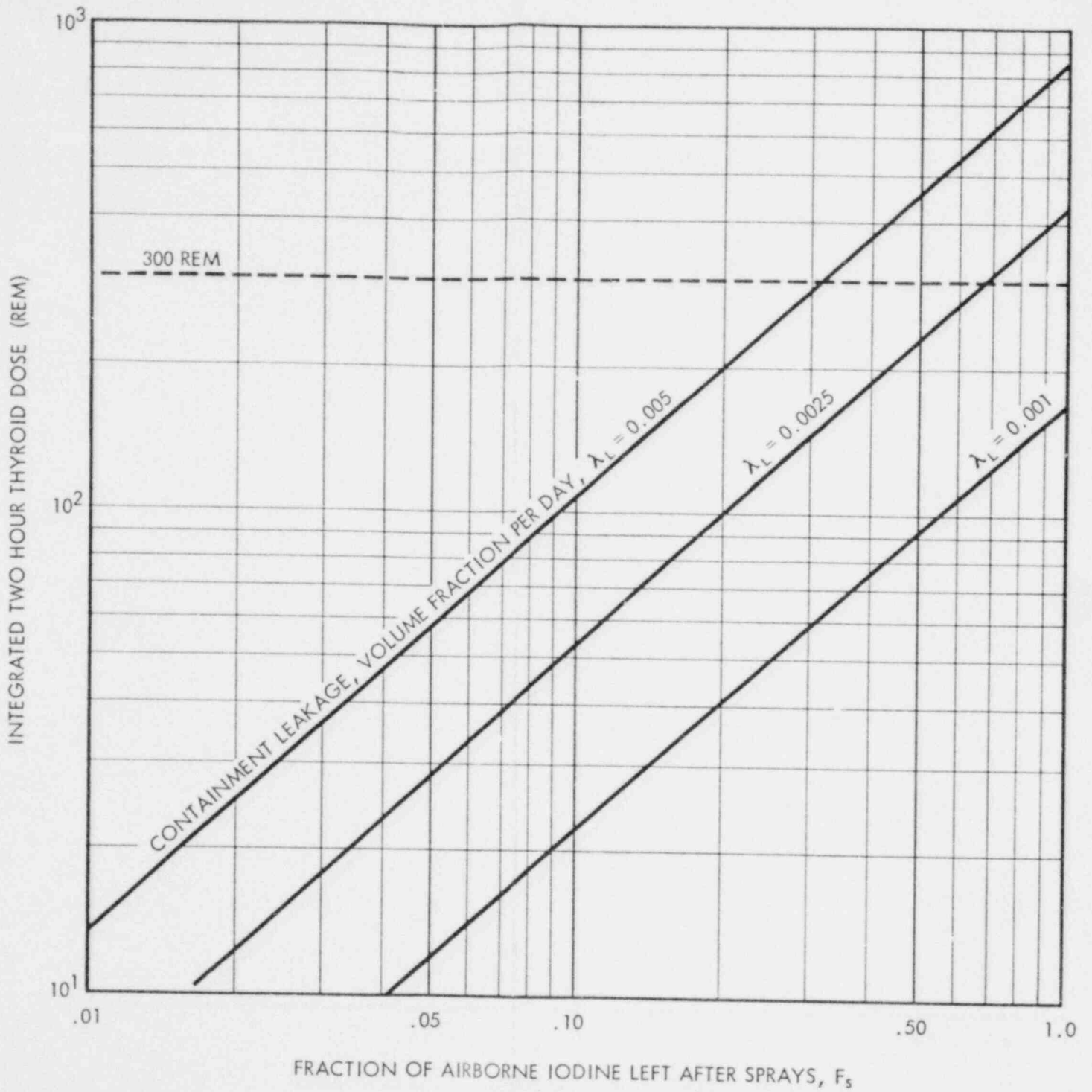
Heat is assumed to be transferred to the steam generator until the reactor coolant inlet temperature to the steam generator reaches 552 F, the saturation temperature at 1,050 psig which is the steam generator safety valve set point. Heat is then transferred from the steam generator through the tubes to the reactor coolant. Heat transfer coefficients were estimated based on the flow in the loop as predicted by FLASH.

Heat transfer to the reactor coolant steam atmosphere after blowdown is over is assumed to take place with a heat transfer coefficient of 2 Btu/hr-ft<sup>2</sup>-F using the total heat transfer surface of the tubes.

For this rupture approximately 9 million Btu are transferred to the steam generator during Stage 1 (15 sec), and approximately the same amount is transferred back over a period of 30 sec. Thus, an energy balance exists at the time the peak reactor building pressure occurs. Continued heat removal from the steam generator between the end of blowdown and the second pressure peak, which is 2.6 psi less than the first peak, is on the order of 0.2 million Btu. The net energy addition to the reactor building during the first 180 sec is less than 1 million Btu and has no effect on the reactor building peak pressure.

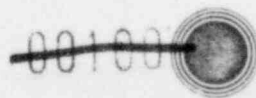
~~00099~~

0183



0184

FIGURE 14A.11-1  
 THYROID DOSE AT THE SITE BOUNDARY  
 AS A FUNCTION OF  $\lambda_L$  AND  $F_s$



**SMUD**

SACRAMENTO MUNICIPAL UTILITY DISTRICT

Amendment 1



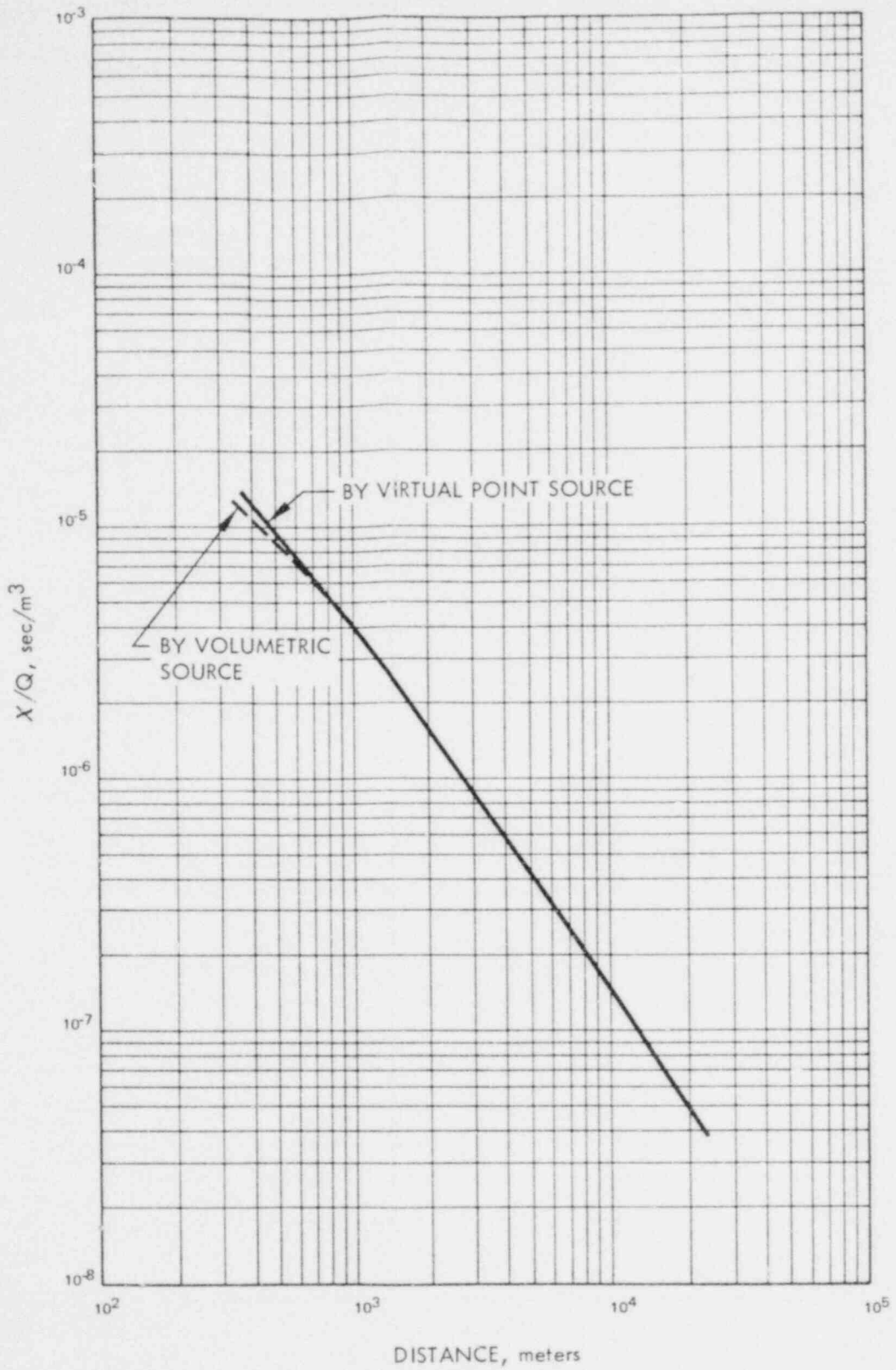


FIGURE 14A.11-2  
LONG - TERM ATMOSPHERIC DILUTION FACTORS

0185



**SMUD**

SACRAMENTO MUNICIPAL UTILITY DISTRICT

~~00101~~

Amendment 1

Core Thermal Transient

The effect of this energy transfer on core cooling is negligible as the energy transfer is small compared to the total in the system. This transfer would be seen as only slight changes in coolant temperature and steam qualities. Since these changes are first in one direction and then reverse during the second portion of the blowdown, compensating effects will occur.

~~00102~~

0183

QUESTION  
14A.13

Calculate the effect on the peak loss-of-coolant accident containment pressure of (1) a steam generator blowdown due to a massive failure during primary system blowdown, and (2) a steam generator blowdown through a number of tubes ruptured during the primary system blowdown.

ANSWER  
14.2

Massive Failure

This analysis was performed for the 3.0 ft<sup>2</sup> rupture of the reactor outlet piping, assuming minimum core injection, i.e., 6600 gpm, and operation of two core flooding tanks and three reactor building emergency coolers. The total mass and energy contained by one steam generator plus feedwater coastdown is 47,500 lbs and  $29.1 \times 10^6$  Btu, respectively.

For the case of massive failure during reactor coolant (primary) system blowdown, it was assumed that the above additional mass and energy was released to the reactor building coincident with the primary pipe rupture. This results in a peak pressure of 58.7 psig which is below the 59 psig design pressure of the reactor building.

Tube Rupture

The second case was analyzed releasing the above additional mass and energy linearly over a period of 2000 sec following the rupture. This is equivalent to the failure of two steam generator tubes. The results of this calculation show virtually no increase (.1 psi) in the peak building pressure. At the time of peak pressure (~40 sec), very little additional energy has been released.

~~00103~~

0187

QUESTION 14A.14 (DRL 2.1) An analysis should be presented which relates primary coolant activity, assumed leakage rate from the primary to secondary system, removal and cleanup mechanisms for the secondary coolant, and the derived activity contained in the secondary system.

ANSWER Reactor Coolant System Activity Levels

Calculation of activity levels in the reactor coolant system resulting from fission product leakage through clad defects was explained in the reply to Question 11A.3 in Amendment 1.

With a 1 gpm leak, fission products contained in the reactor coolant system leak into the secondary side of the steam generator at the following rates:

<u>Isotope</u>	<u>Leak Rate μc/Sec</u>	<u>Isotope</u>	<u>Leak Rate μc/Sec</u>
Kr 85M	94.7	I 131	202.
Kr 85	618	I 132	297.
Kr 87	53.0	I 133	240.
Kr 88	170.	I 134	31.6
Rb 88	170.	I 135	170.
Sr 89	2.59	Cs136	48.0
Sr 90	0.18	Cs137	1640.
Sr 91	2.90	Cs138	46.7
Sr 92	1.07	Mo 99	341.
Xe131M	126.	Ba139	5.11
Xe133M	170.	Ba140	4.10
Xe133	15300.	La140	1.33
Xe135M	59.3	Y 90	16.4
Xe135	353.	Y 91	11.4
Xe138	32.2	Ce144	0.170

At the leakage rates postulated above, approximately  $1.7 \times 10^4$  μci/sec of noble gases will be released without retention to the atmosphere through the steam condenser air ejector. Stack monitor alarms will give warning if the noble gases release rate will exceed a predetermined level which could result in downwind concentrations exceeding (MPC)<sub>a</sub> values.

Since approximately one-half of the condensate flow leaving the steam condenser will pass through the polishing demineralizers, the non-gaseous fission products will be removed from the

0188

~~00104~~

condensate and retained on the resin beds, leaving an overall activity level in the secondary coolant estimated at less than 0.005  $\mu$ ci/ml.

QUESTION 14A.15 (DRL 2.2) The PSAR description of the steam generator tube accident includes an assumption that the iodine water to air partition factor is 10,000. Show how this factor was derived, and indicate how concentration, temperature, pressure, and air to water volume ratio which exist throughout the course of the accident may affect this partition factor.

ANSWER Table 14A.15-1 shows the general effects of the listed parameters, the specific effects on fuel handling accident, and specific effects on steam generator tube rupture accident conditions. A comparison of the conservatism of the experimental conditions of the referenced experimental data with those of a fuel handling accident are tabulated in Table 14A.15-2. These tables indicate that the experimental data has been conservatively applied.

The partition coefficient under the conditions of a fuel handling accident and of a steam generator tube rupture accident are orders of magnitude higher than those used in accident analysis. (Figures 14A.15-1 and 14A.15-2)

#### References

1. Watson, et.al., "Iodine Containment by Dousing in NPD-11" AEC-1130 1960
2. Styrickovich, M. A. et.al., "Transfer of Iodine from Aqueous Solutions to Saturated Vapor", Soviet Journal of Atomic Energy, Vol. 17, June-Dec. 1965, p.735.
3. Stinchcombe, R. A. and P. G. Goldsmith, "Removal of Iodine from the Atmosphere by Condensing Steam", Journal of Nuclear Energy, Parts A/B, Vol. 20, pp 261-275, 1966.
4. Barthoux, A., J. Couland, R. Havlet, "Diffusion of Active Iodine Through Water, with the Iodine Being Liberated in CO<sub>2</sub> Bubbles at High Temperatures". AEC-TR-6149. June 1962.
5. Diffey, H. R., et.al., "Iodine Clean-up in a Steam Suppression System" AERE-R-4882, May 1965 and p 776 in Proceedings of the International Symposium on Fission Product Release and Transport Under Accident Conditions, Oak Ridge, Tennessee, April 5-7, 1967, (USAEC Rept. Conf. 65047).
6. Eggleton, A. E. J., "A Theoretical Examination of Iodine-Water Partition Coefficients" AERE-R-4887 Feb. 1967.

~~00105~~

Condition No.	Parameter	General Effect & Reference
1	pH	In high concentrations of iodine in water the pH, the higher the partition coefficient. At low concentrations the pH becomes less above a critical value determined by the (4)
2	Temperature	The effect of temperatures is dependent on concentration. When the concentrations are high volatility increases with temperature in water. When the concentrations are very low it is hydrolysis. But lower temperatures always reduce the volatility and reduce the release of iodine from the pin gap. (2) (4).
3	Pressure	The effect of pressure is dependent on the concentration of the solution (4).
4	Concentration	In high concentrations the partition coefficient is in agreement with predictions based on Henry's Law (Viz. 70). It increases rapidly as the concentration of iodine in water decreases below 1 liter. Partition factors $>10^4$ are commonly reported. (1) (2) (3) (4) (5).
5	Water Volume to Carrier Gas Volume Ratio	Higher water volume to total gas bubble produces higher partition coefficients. The volume of air above is not as important as the volume of iodine is hydrolyzed passing through the pin gap. (3) (5).

0130

~~00106~~

TABLE 14A.15-1

IOUS CONDITIONS ON IODINE PARTITION FACTORS

	Fuel Handling Conditions	Steam Generator Tube Rupture
<p>er, the higher cient. In significant e concentration.</p> <p>on the con- e high, solu- nge 0°-60°C. enhances ays decrease rom the fuel</p> <p>the pH range</p> <p>ctor is in ry's Law e concentra- v 10<sup>-4</sup>g mole/ only</p> <p>e volume . The t if the ne pool.</p>	<p>The pH of the water pool is slight- ly acidic from the boric acid. This means that the partition factor is slightly less than for a neutral solution. But in concentration range of fuel handling accident, this effect is not significant.</p> <p>The temperature of the water is always &lt;140°F. This precludes boiling and the lower volatility of iodine at this temperature reduces the release. The hydroly- sis rate at these temperatures and concentrations is high.</p> <p>Not applicable, since changes in pressure do not occur.</p> <p>The concentrations of iodine in water is limited to &lt;10<sup>-3</sup>g Iodine/liter. (Based upon approximately one half the volume directly above the fuel assembly.) Insufficient iodine is available for release to permit higher concentrations.</p> <p>The Water volume is very much greater than the total gas volume released through it and almost complete hydrolysis of the iodine occurs.</p>	<p>pH is ~ 9.0 - 9.5. Tends to increase partition factor.</p> <p>See Figure 14A.15-2</p> <p>No appreciable change from data in Figure 14A.15-2.</p> <p>Concentration is &lt;&lt;10<sup>-9</sup>g/l. All iodine is hydrolyzed.</p> <p>Iodine is already completely hydrolyzed before accident. This makes the volume ratio less important since hydrolysis apparently inhibits re-establish- ment of equilibrium partition factors and the aqueous phase tends to retain a greater portion of iodine than it would under equilibrium conditions.</p>

~~00107~~

0191

Fuel Handling Accident

Conservatism of Experiment vs Assumed

Analytical Conditions

TABLE 14A.15-2

Parameter	Reference No.					Static Conditions	
	1	2	3	4	5	Henry's Law	(4) Bett's
Concentration	P	✓	+	(-)	✓	(-)	(-)
Impurities	+	(-)	+	(-)	✓	(-)	(-)
Water to Gas Ratio	(-)				(-)	(-)	(-)
Height	(-)			✓	(-)		
Bubble Size					(-)		
Carrier					(+)		
Temperature			✓		✓	✓	
Flow Rate		P		(-)	(-)		
pH		✓			✓		(-)
Pressure	P	P			✓	✓	
Partition Factor	10 <sup>4</sup>	10 <sup>2</sup>	10 <sup>4</sup>	10 <sup>2</sup> to 10 <sup>6</sup>	10 <sup>3</sup>	60 - 80	108

✓ : Applicable

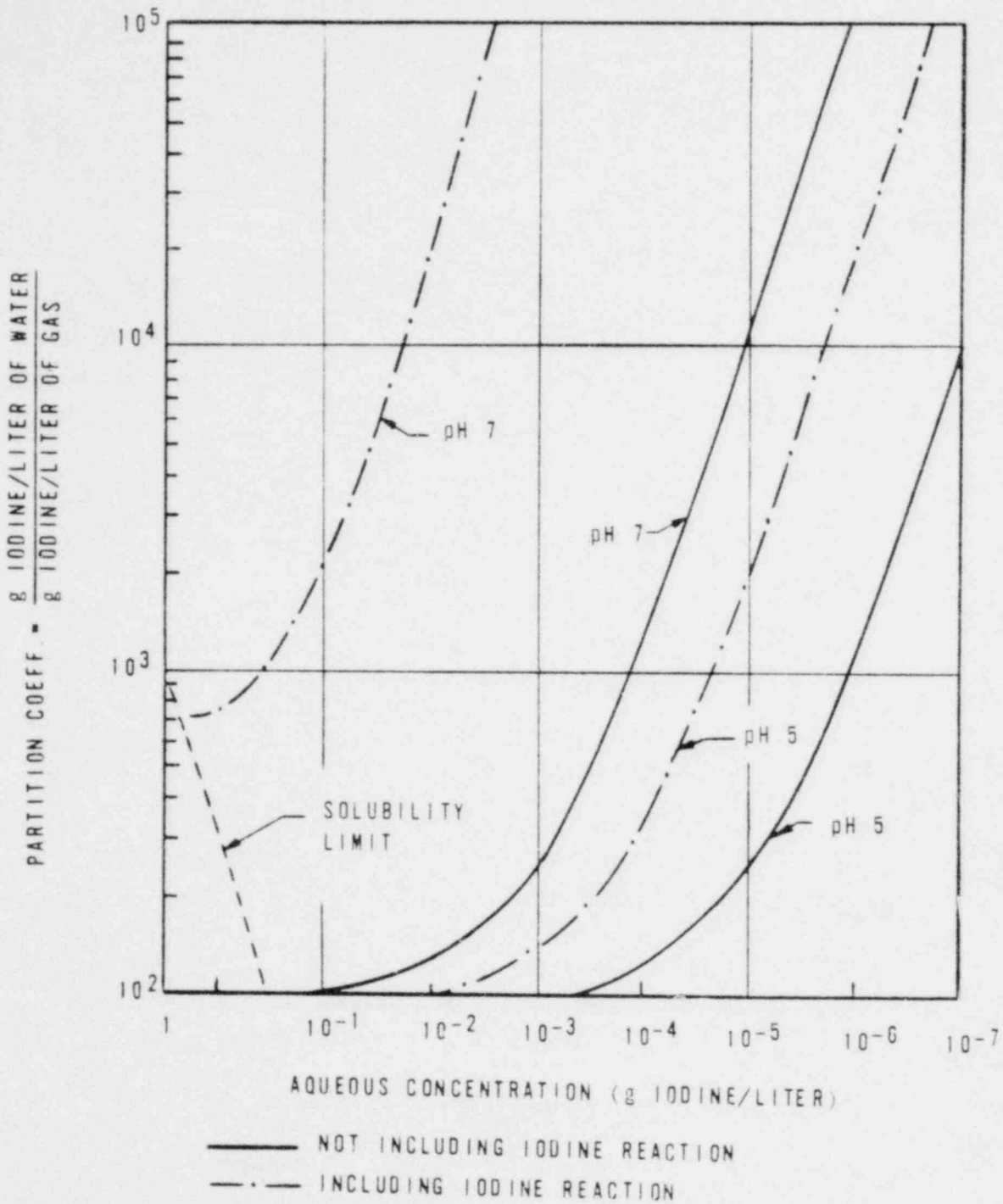
(-) : Indicates test conditions were less favorable for iodine partition as compared to accident condition.

(+) : Indicates test conditions were more favorable as compared to accident condition.

P : Parametric study.

~~00108~~





NOTE: pH OF FUEL HANDLING PIT WATER IS  $\geq 5$  AND CONCENTRATION IS  $\ll 10^{-3}$  g IODINE/LITER

0193

FIGURE 14A.15-1  
 PARTITION OF IODINE BETWEEN GAS  
 PHASE AND WATER AT 25 C (6)

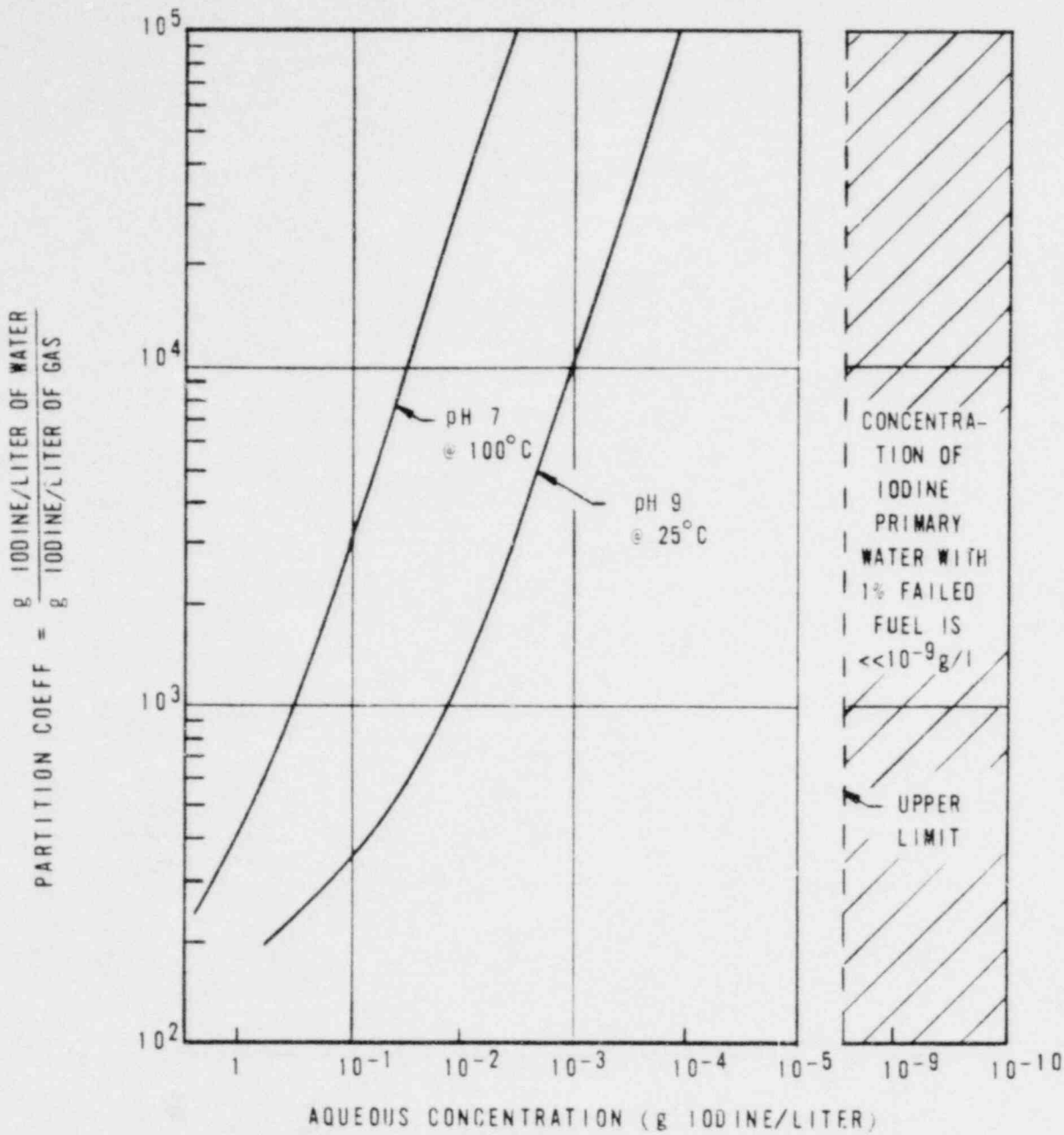
~~00109~~



**SMUD**

SACRAMENTO MUNICIPAL UTILITY DISTRICT

Amendment 3



NOTE: THE pH 9 @ 100°C LINE IS A CONSERVATIVE APPROXIMATION OF CONDITIONS OF STEAM GENERATOR TUBE RUPTURE.

~~00110~~

FIGURE 14A.15-2  
PARTITION OF IODINE BETWEEN  
GAS PHASE AND WATER (6)

0194

QUESTION 14A.16 (DRL 2.3) The PSAR calculations of off-site doses due to release of noble gases include an assumption that the average effective energy per disintegration of noble gases is 0.4 Mev. The origin or justification of that assumption should be provided.

ANSWER The average gamma ray energy of the noble gases  $\bar{E}$ , Mev., had been calculated as a function of time, t sec, according to the method outlined in "Review of Modern Physics", Vol. 30, No. 2, April 1958:

$$\bar{E}(t) = \frac{\sum_i \bar{E}_i A_i(t)}{\sum_i A_i(t)}$$

where the activity  $A(t) = A_0 e^{-\lambda t}$  dis/sec;  $A_0$  is the isotopic activity at  $t = 0$ , and  $\lambda_i$  is the isotopic radioactive decay constant.

The average gamma ray energies of noble gases calculated by the formula above were applied in the exposures resulting from accidents involving coolant or gap activity releases. The average gamma ray energy of the gap activity during the first two hours after the release is approximately 0.130 Mev., and drops to about 0.110 Mev. considering long-term (30 day) releases. The dominant contribution is from Xenon-133 which has a gamma energy of 0.081 Mev. To be conservative, an average gamma ray energy of 0.4 Mev. was used in the dose evaluation at all downwind distances in accidents involving coolant or gap activity releases. However, cloud doses from the MHA were computed by adding contributions from individual isotopes rather than using an average value.

The average  $\beta$  energy of the airborne fission products following a release of primary coolant or fuel gap activities is approximately 0.14 Mev for the first 200 hours rising to 0.22 Mev at about 1000 hours at which time the  $\beta$  activity is essentially that of Krypton 85 with  $\bar{E}_\beta = 0.222$  Mev. As indicated, at the same time the average  $\gamma$  activity of these fission products is approximately 0.110 Mev, a value of 0.4 Mev was assumed for the dose calculations. It is believed that in this way enough conservatism was introduced in the calculations of whole-body doses from deep penetrating radiation to provide for any possible contribution from  $\gamma$  in addition to  $\beta$  activities.

The average  $\gamma$  and  $\beta$  isotopic activities used in the dose computations to arrive at an average cloud value are those listed in the ICRP "Report of Committee II on Permissible Doses for Internal Radiation." The isotopes considered are as follows:

3

~~00111~~

0135

<u>Isotope</u>	<u>Gamma Energy</u>	<u>Beta Energy</u>	<u>Isotope</u>	<u>Gamma Energy</u>	<u>Beta Energy</u>
I 131	.4	.191	Kr 87	1.067	1.0375
I 132	2.115	.458	Kr 88	2.069	.331
I 133	.660	.414	Xe 131m	.164	0
I 134	2.381	.573	Xe 133m	.233	0
I 135	2.167	.305	Xe 133	.081	.115
Kr 83m	.050	0	Xe 135m	.53	0
85m	.18	.222	Xe 135	.264	.300
Kr 85	.005	.222	Xe 138	.420	.80

Activities postulated as released into the Reactor Building following DBA, are the total gap and coolant activities. The gap activity is the dominant activity and is indicated in the PSAR, Sec. 14.2, page 14.2-38. The cloud activity resulting from building leakage assumes a spray removal of iodine, as postulated in the PSAR for this accident. Cs isotopes and other particulate fission or corrosion products which may be released from coolant are assumed to be removed totally in the Reactor Building. Consequently, the cloud activity corresponds essentially to that of noble gases and iodine remaining airborne in the Reactor Building after sprays.

~~00112~~

0196

QUESTION  
14A.17  
(DRL 2.4)

Submit a listing of the radioactive isotopes and maximum activities of each which may be present in the liquid waste holdup tanks at any one time, and include an analysis demonstrating that failures in the liquid waste system would not cause excessive release of radioactive liquids to the environs.

ANSWER

The most severe liquid waste tank accident would be a sudden splitting apart of the tank, releasing all liquid on the concrete pad under the tank. The raised border around the pad will be high enough to hold all liquid on the pad until the drain normally closed is open and the liquid is allowed to drain into the dirty liquid waste system. After purification, the liquid will be eventually returned to the primary system.

Radioactivity contained in the liquid is primarily that of the dissolved noble gases. All other fission products and activated corrosion products are retained on the ion exchangers ahead of the liquid waste tank. During normal operations, air is passed continuously through the liquid waste tank over the surface of the liquid. Very small amounts of the noble gases dissolved in the liquid diffuse from the liquid and are carried with the air stream to the stack. Although reliable experimental data on these diffusion rates are lacking, such information is anticipated to be forthcoming from the operation of existing stations.

Since the pressure and temperature inside and outside of the liquid waste tank are approximately equal, splitting apart of the tank and the spillage of the liquid on the concrete pad will not alter the driving force of the diffusion process except for a certain increase in the exposed liquid-air interface and a decrease in air flow over the liquid surface. Therefore, it is not anticipated that a noble gas release from the spilled liquid surface will increase in any significant manner compared to normal operations.

However, even if some radioactivity was released in this accident from the spilled liquid to the auxiliary building atmosphere, the ventilation system of this building would prevent any significant buildup of noble gases in the working areas.

Although it is evident from the discussion above that a liquid waste tank rupture will not result in an increase of downwind concentration of noble gases, a calculation was performed to evaluate downwind doses if it is postulated that all noble gas activity in the liquid waste gas tank is suddenly released to the atmosphere. The calculation assumes that the xenon and krypton activity in the liquid waste tank is the same as in the primary coolant (no decay). The activities of noble gases in the primary coolant, based on 3rd core cycle and 1% of fuel elements failed, are indicated in the PSAR, Section 11, Table 11.1-3. Since the liquid waste tank holds a maximum of 8,000 ft<sup>3</sup> of liquid and if all noble gas activity in the liquid is instantaneously released to the atmosphere, the airborne isotopic amounts would be as follows:

0197

Kr 85m	-	340 curies	Xe 131m	-	452 curies
Kr 85	-	2,210	Xe 133m	-	610
Kr 87	-	190	Xe 133	-	55,000
Kr 88	-	610	Xe 135m	-	212
			Xe 135	-	1,270
			Xe 138	-	115

The whole-body gamma ray dose at the site boundary resulting from this activity is 0.3 rem.

The above value should be regarded only as a mathematical exercise to demonstrate that a whole body dose from a total release of activity from a split liquid waste tank would result in a relatively small whole body doses at the site boundary. However, no physical mechanism is known to exist or can be credibly postulated for such a release.

~~00114~~

0198

QUESTION 14A.18 (DRL 2.5) Specify the distance to the low population zone as it is defined in 10 CFR Part 100, Section 100.3 (b).

ANSWER The distance to the boundary of the low population zone has been selected as five (5) miles.

Selection of the 5 mile radius was on the basis of the following considerations:

1. Calculated radiation exposure to the thyroid resulting from postulated releases.
2. Proximity of population concentrations and institutional facilities.
3. Data developed for Emergency Evacuation Plan (Ref. question 12A.8).

In order to determine the range of 0-30 day thyroid exposure that might be experienced as a result of a Maximum Hypothetical Accident, two cases were analyzed.

The first case was that in which the MHA was assumed to occur with the iodine spray removal system operating (20% of the iodine left airborne in Reactor Building after sprays). The second case was that in which the spray system was assumed not to be operating subsequent to the MHA, and thus providing an upper limit to thyroid doses.

Results of these analyses show that under the criteria of 10 CFR 100.11, the low population boundary may be set at 1.19 miles from the site (no credit for spray). A comparison of the two cases analyzed is shown on Figure 14A.18-1.

A survey of the area contiguous to the plant shows that the nearest population concentration of untractable size to be approximately 6.5 miles from the plant site. A summary of institutional facilities showing function and location is shown in Table 14A.18-1.

As may be seen in the summary presented in Table 14A.18-2, a 5 mile low population zone provides adequate protection for public safety and insures a reasonable probability that appropriate protective measures can be taken in their behalf in the event of serious accident.

0159

~~00115~~

TABLE 14A.18-1

LIST OF INSTITUTIONS  
WITHIN A 10-MILE-RADIUS OF RANCHO SECO

1. Altura Village for T.B. & Alcoholic Patients (50 units)	6-1/2 miles
2. Home for Aged (15 units)	6-1/2 miles
3. Arcohe Union Elementary School	7 miles
4. Dillard Elementary School	8-1/2 miles
5. Home for Aged	9 miles
6. Preston School of Industry (Calif. Youth Authority)	10 miles
7. Ione High School	10+ miles
8. Ione Elementary School	10+ miles

TABLE 14A.18-2

Location	Calculated Per 10CFR100.11		Established Per 10CFR100.3
	W/Spray	W/O Spray	
Low Population Zone Boundary	500 Meters (Inside Site Boundary)	1.19 Miles	5.0 Miles
Population Center Distance	605 Meters (Inside Site Boundary)	1.58 Miles	17.0 Miles

~~00116~~

0200



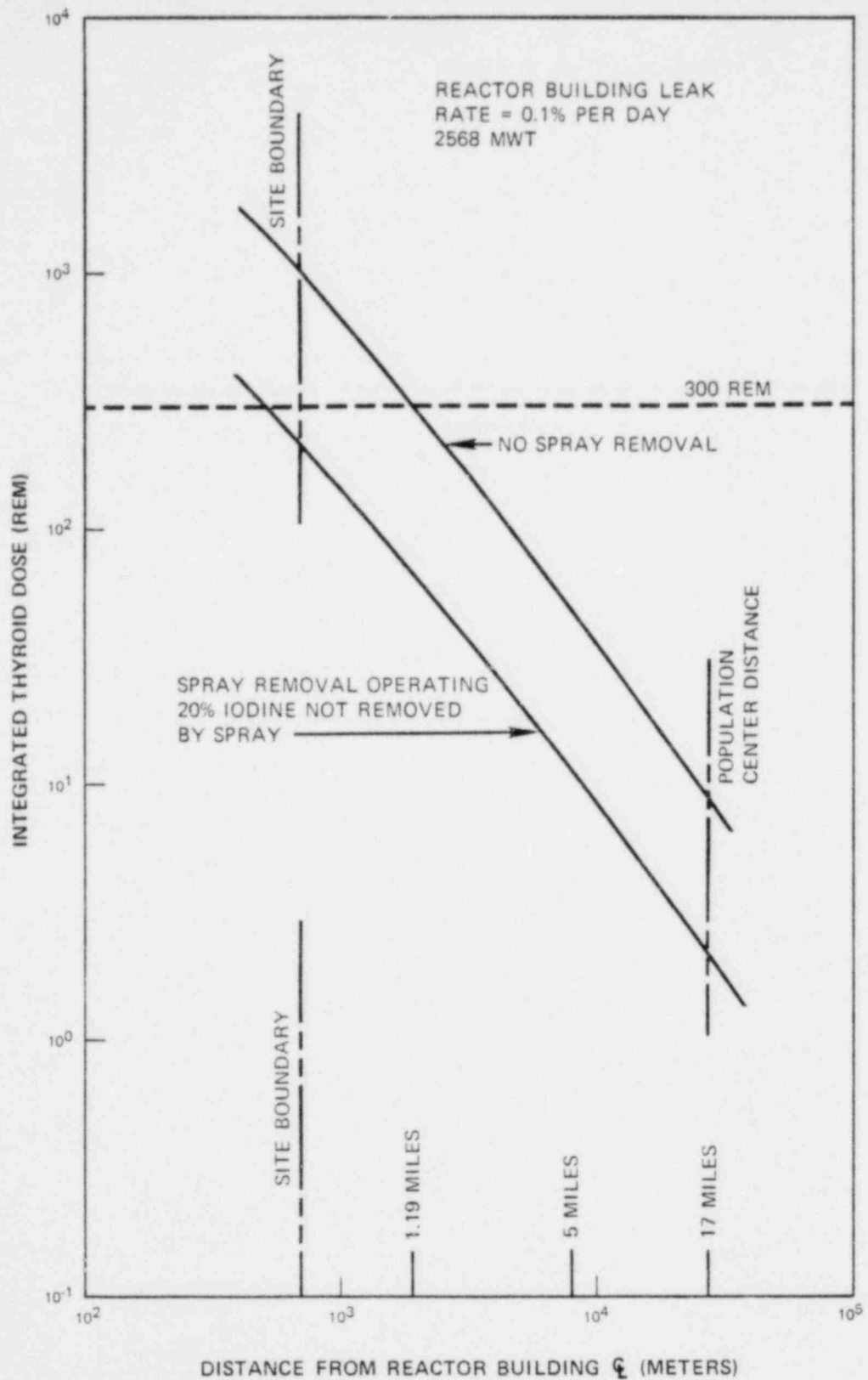


FIGURE 14A.18-1  
INTEGRATED THYROID  
DOSE 0-30 DAY

0201



**SMUD**

SACRAMENTO MUNICIPAL UTILITY DISTRICT

~~00117~~

QUESTION 14A.19 (DRL 2.6) Based on data presented in the PSAR, it appears that the Rancho Seco site is subjected to a high frequency of inversion conditions with low transport winds. Data presented show a computed frequency of about 25% extremely stable conditions with an average wind speed of 0.9 meters per second; it would appear appropriately conservative to use this condition for calculating the 2 hour off-site doses. Please provide the environmental consequences of hypothetical accidents using this basis.

ANSWER Doses to the thyroid at the site boundary, following the Maximum Hypothetical Accident, computed for stability class G and a wind speed of 0.9 m/sec., are shown in Figure 14A.19-1. The values of  $\sigma_y$  for class G were obtained from Figure 21 of Appendix 2A. For comparison purposes, doses under class F (wind speed 2.0 m/sec) and class E (4.2 m/sec) are also shown. The doses are plotted as a function of the fraction of the released iodine remaining airborne in the Reactor Building after chemical additive sprays and are based on 0.1% per day leakage.

From the results of recently collected on-site meteorological data (Appendix 2A, Supplemental Report) it is observed that condition G and 0.9 meters per second wind speed has a frequency of occurrence of only 5 percent. Hence, all the hypothetical accidents for G and 0.9 m/sec were not calculated, since the consequences of the Maximum Hypothetical Accident presented demonstrate the safety of the site even under the worst possible combination of meteorological parameters.

~~00119~~

0202

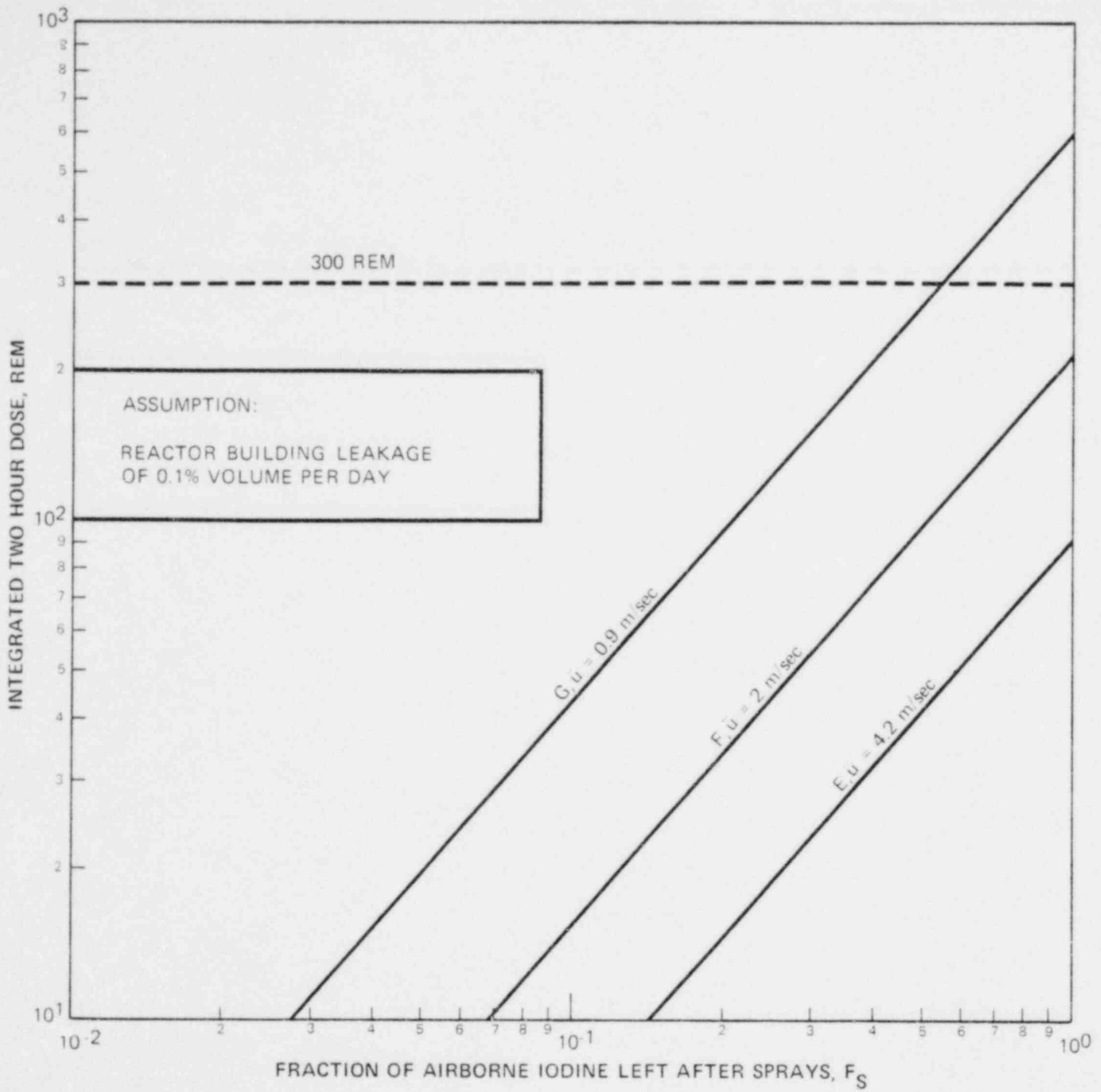


FIGURE 14A.19-1  
 THYROID DOSE AT THE SITE BOUNDARY  
 AS A FUNCTION OF  $F_S$  AND METEOROLOGY

0203

00119



QUESTION Describe the analytical model used to study the reactor system  
14A.20 response to a 100% loss of demand and to total loss of a.c.  
(DRL 14.1) power.

ANSWER The analytical model used to study reactor system response to  
loss of demand load is an analog model. The model contains:

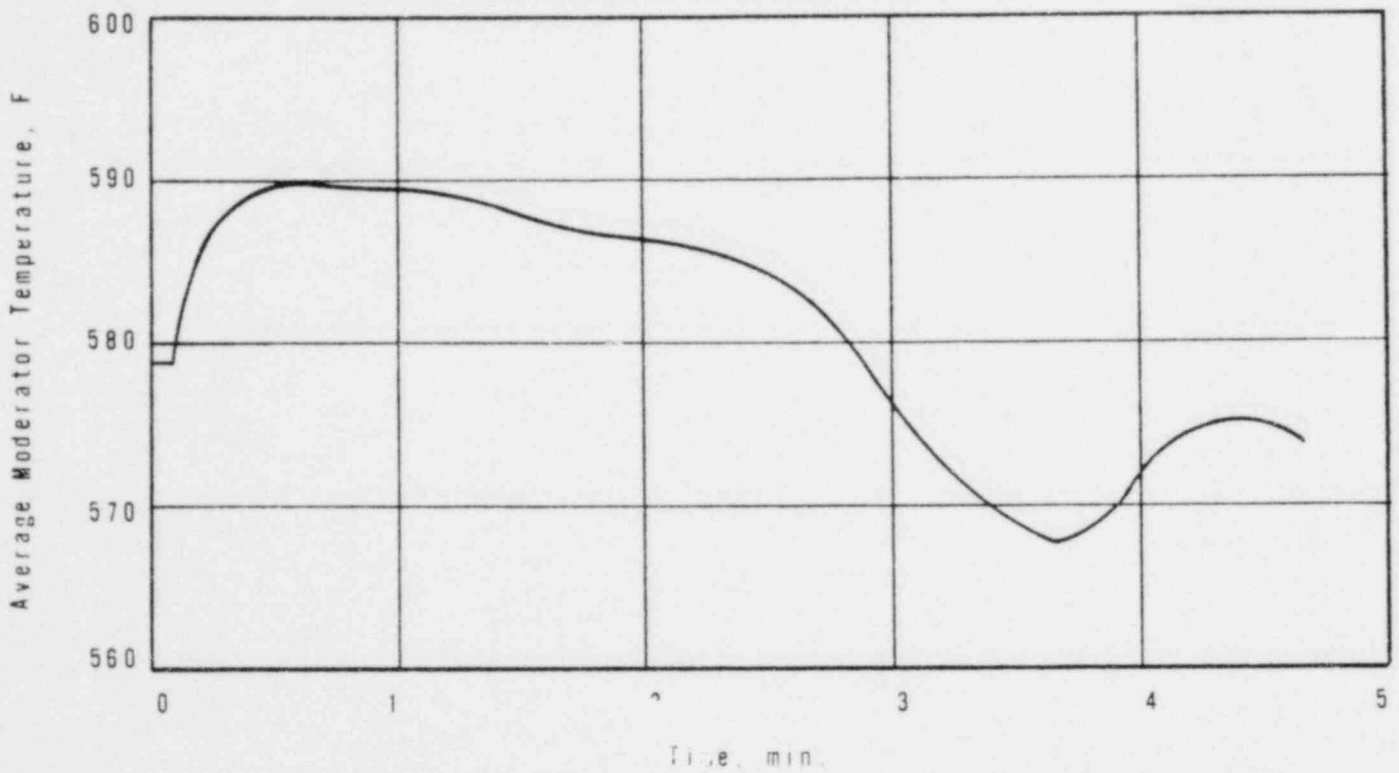
- (1) kinetics simulation with delay groups
- (2) fuel pin heat transfer
- (3) transient and mixing delays from reactor to steam generator
- (4) pressurizer, including heaters, spray, and relief valves
- (5) steam generator
- (6) feedwater system
- (7) steam system with turbine simulation, turbine bypass and steam relief valves.

The flow transient following total loss of a.c. power is analyzed with a separate analog model which incorporates hydraulic characteristics of each loop and the zone maps for each pump.

DNB ratios during transients are calculated with the transient thermal-hydraulic digital computer code discussed on page 14.1-11 of the PSAR.

~~00120~~

0204



0205

FIGURE 14A.21-1  
 AVERAGE MODERATOR  
 TEMPERATURE VERSUS TIME

~~00121~~



**SMUD**

SACRAMENTO MUNICIPAL UTILITY DISTRICT

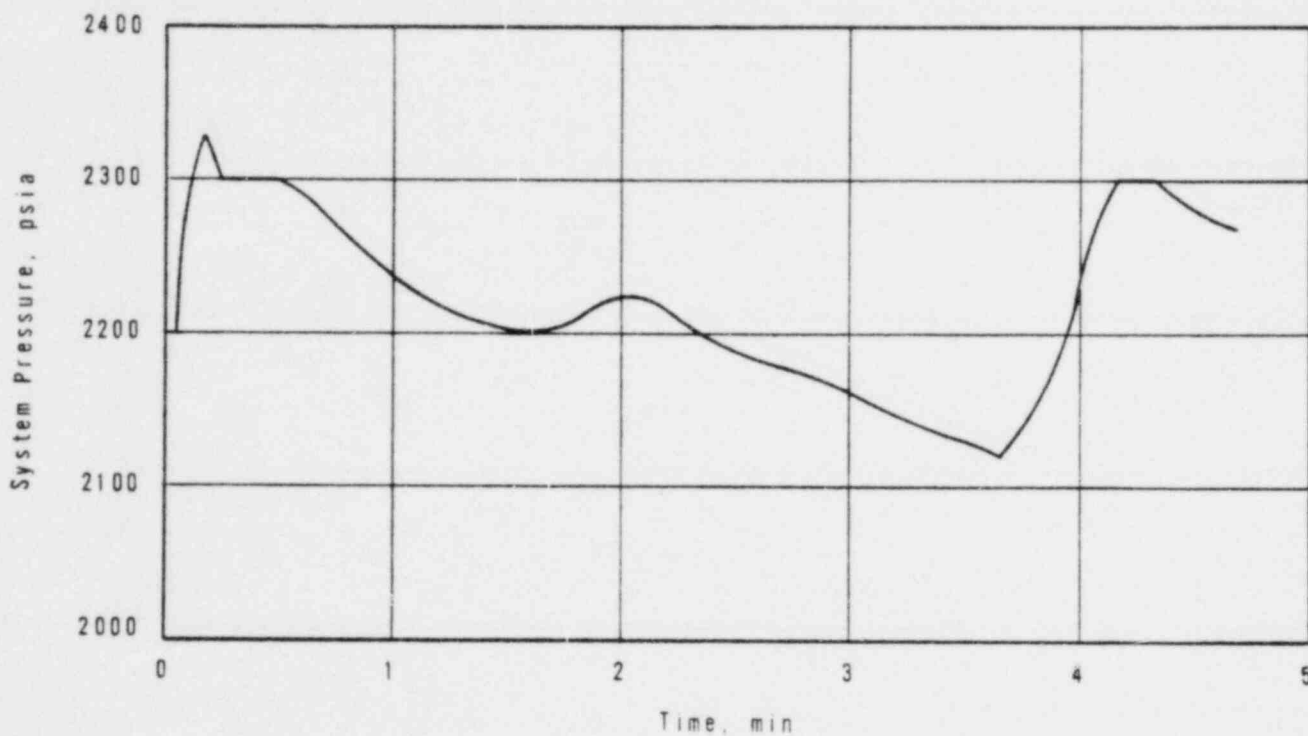


FIGURE 14A.21-2  
SYSTEM PRESSURE VERSUS TIME

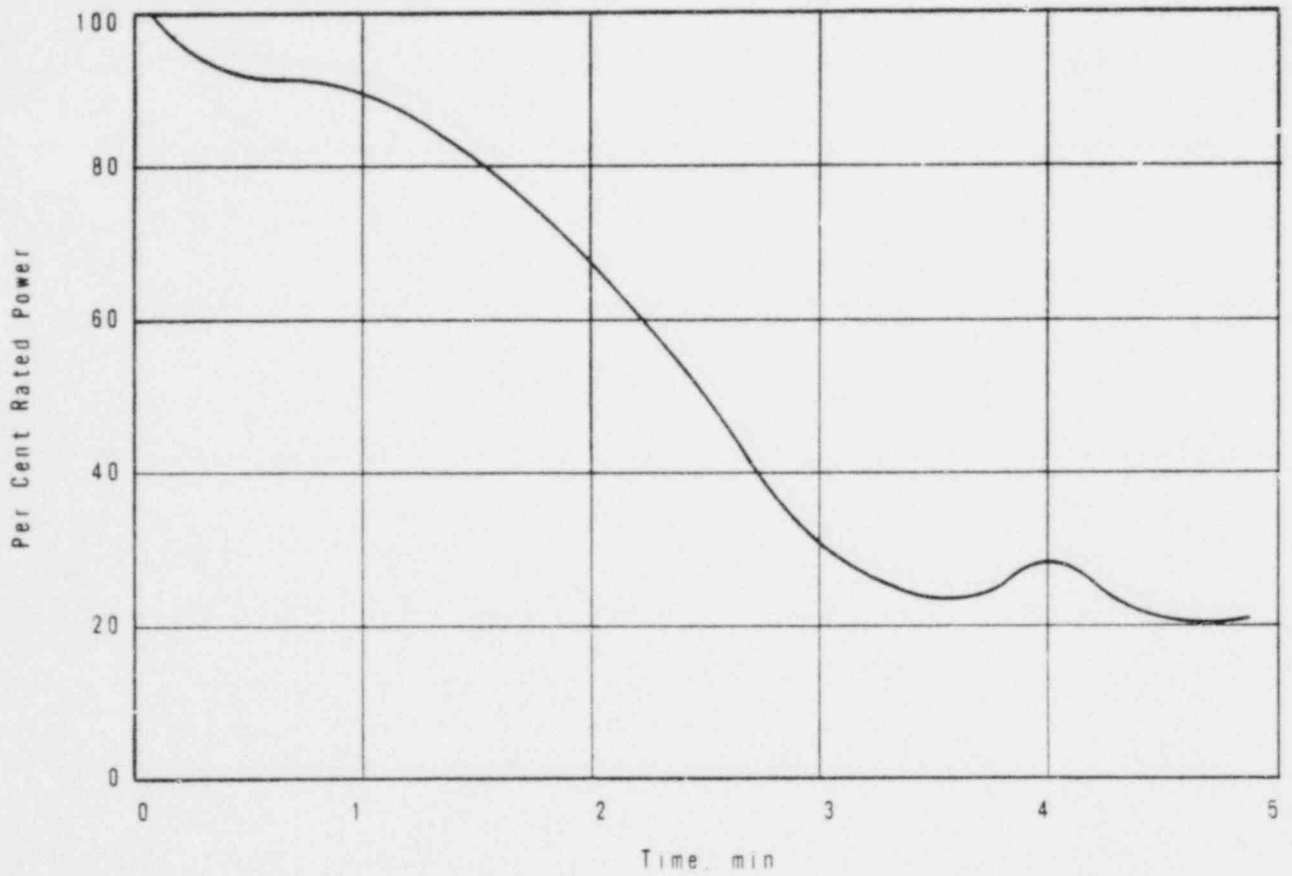
0206



**SMUD**

SACRAMENTO MUNICIPAL UTILITY DISTRICT

~~00122~~



0207

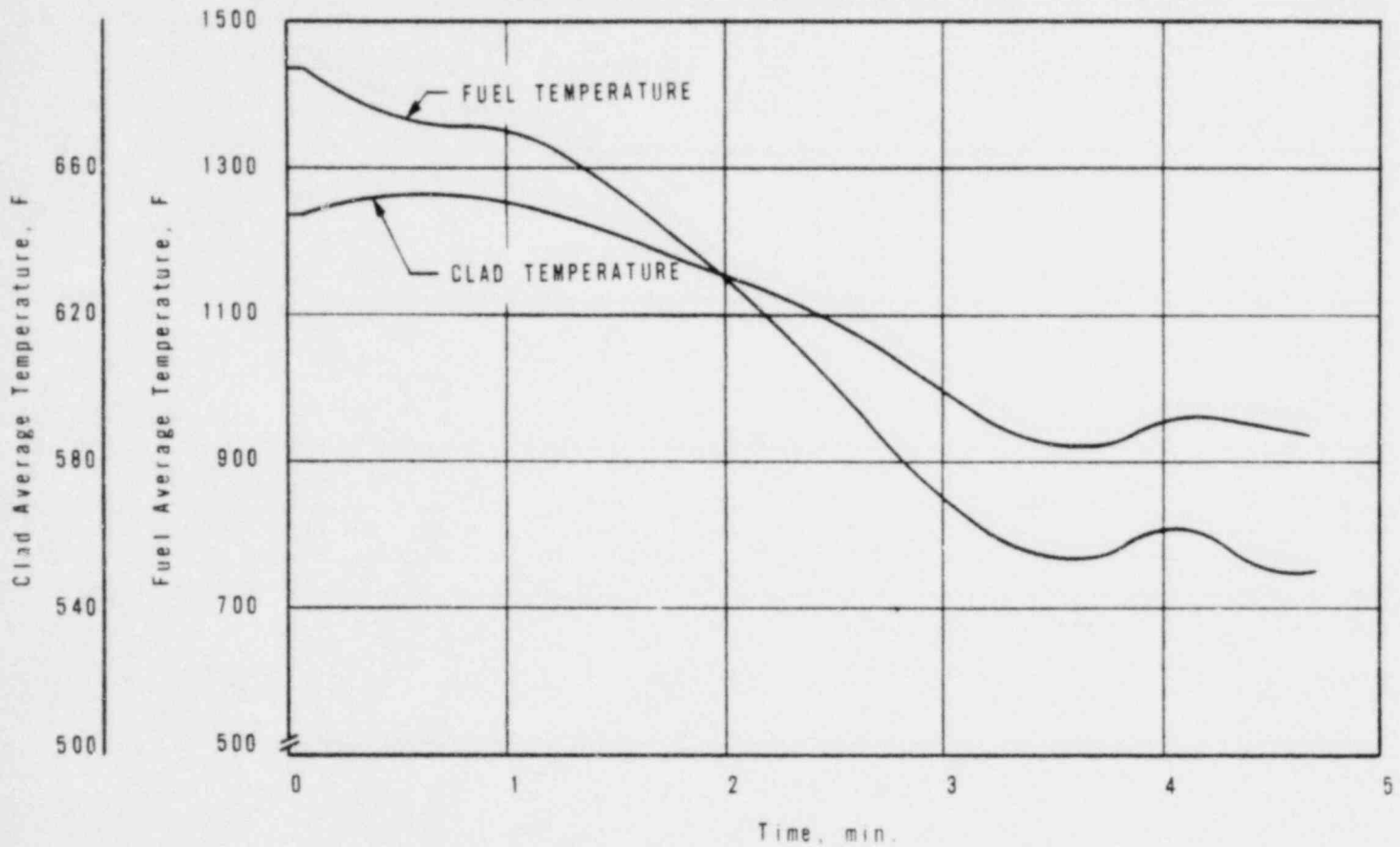
FIGURE 14A.21-3  
 REACTOR THERMAL  
 POWER VERSUS TIME

~~00123~~



**SMUD**

SACRAMENTO MUNICIPAL UTILITY DISTRICT



0208

FIGURE 14A.21-4  
 FUEL AVERAGE TEMPERATURE  
 AND CLAD AVERAGE TEMPERATURE  
 VERSUS TIME, AVERAGE FUEL PIN



**SMUD**

SACRAMENTO MUNICIPAL UTILITY DISTRICT

00124



QUESTION 14A.22 Describe the natural circulation characteristics of the primary loop system. Will operation of primary loop relief valves, due (DRL 14.3) to its deadband characteristics, affect this flow?

ANSWER Figure 14A.22-1 shows the natural circulation flow characteristics of the reactor coolant system as a function of power level.

It is not expected that the deadband characteristics of primary loop relief valves will affect natural circulation flow.

QUESTION 14A.23 In Figures 14.2.1 through 14.2.11 of the PSAR, the reactor kinetic parameters are given for  $\alpha_d$ ,  $\alpha_M$ ,  $l^*$  and  $\tau$ . What were (DRL 14.4) the corresponding values for  $\beta_{eff}$ ?

ANSWER The value for  $\beta$ (effective) for BOL is 0.0071 and for EOL is 0.0053.

QUESTION 14A.24 Discuss the technique used in calculating the effective delayed neutron fraction and include a summary of your calculations for (DRL 14.5) the end-of-life value.

ANSWER In calculating the  $\beta_{eff}$  of the design core, the values found in Table 1-16, ANL-5800 Second Edition were used.

The  $\beta$  for each fissionable isotope was weighted by the power produced by that isotope over the core. The power fractions were taken from a one-dimensional radial lifetime calculation.  $\beta_{eff}$  was calculated for BOL and EOL of cycle I and EOL of cycle IV.

BOL Cycle I  $\beta_{eff}$  = .0071

EOL Cycle I = .0057

EOL Cycle IV = .0053

Although the minimum value for  $\beta_{eff}$  is calculated to be 0.0053 for the core with a maximum burnup, the analysis of the rod ejection accident has been done for values of  $\beta_{eff}$  ranging down to 0.0030.

0209

~~00125~~

An additional evaluation of  $\beta_{\text{eff}}$  has been completed using the following scheme.

- (1) Calculate the delayed neutron fraction at birth energies.
  - (2) Consider the effect of prompt neutrons being born at higher energy than the delayed neutrons and having a greater chance of undergoing fast leakage and fast fission than one lower energy delayed neutrons.
- (1) In calculating  $\beta$  the maximum number of fissions from plutonium was assumed. The table below shows  $\beta$  for each isotope and the fraction of power from each isotope.

<u>Nuclide</u>	<u><math>\beta</math></u>	<u>% Power</u>
U-235	.0065	28%
U-238	.0157 (fast fission)	7%
Pu-239	.0021	65%

$$\beta = \beta^{35} (\% \text{ power})^{35} + \beta^{38} (\% \text{ power})^{39} + \beta^{39} (\% \text{ power})^{39}$$

$$\beta = .0043$$

$$(2) \quad \beta_{\text{eff}} \approx \beta \left[ \frac{\epsilon_D}{\epsilon_P} \cdot \frac{1 + T_P B^2}{1 + T_D B^2} \right]$$

$$\approx 0.004$$

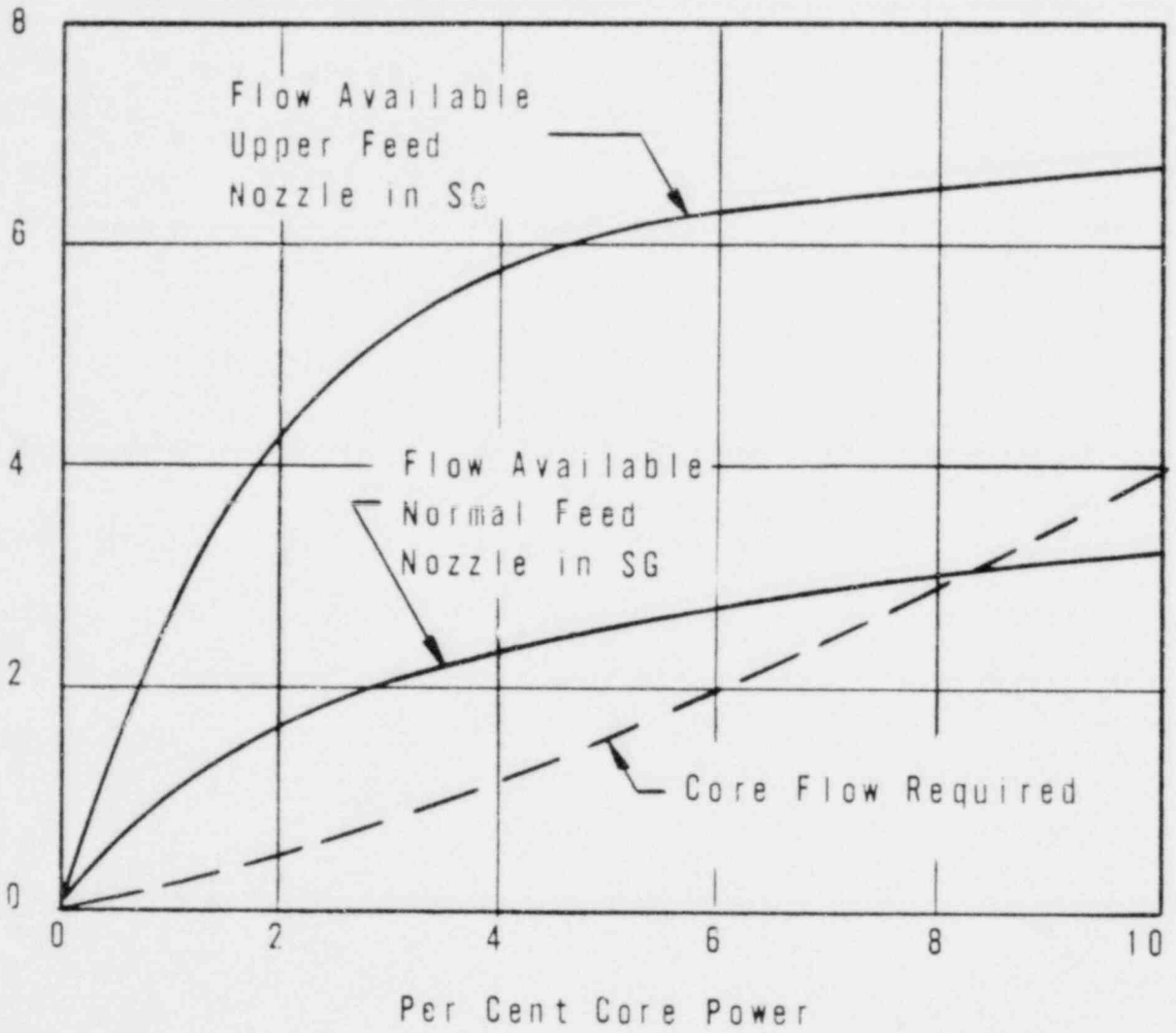
This newer treatment was done for the fuel which has experienced the maximum allowable burnup. This fuel would never occur in the core in large quantities by itself, but would always be surrounded by fuel with much less burnup, therefore this result does not represent a macroscopic parameter as used in any safety analysis, but rather a minimum below which no part of the fuel would ever operate.

This minimum value of  $\beta_{\text{eff}}$  is still much larger than that considered in the rod ejection accident analysis.

0210

~~00126~~

Natural Circulation Flow, per cent design flow



0211

FIGURE 14A.22-1  
REACTOR COOLANT SYSTEM  
NATURAL CIRCULATION  
CHARACTERISTICS

~~00127~~



**SMUD**

SACRAMENTO MUNICIPAL UTILITY DISTRICT

QUESTION 14A.25 Discuss the accuracy of the energy yield predictions for the rod ejection accident. Your discussion should include the (DRL 14.6) anticipated power profile transients.

ANSWER The energy deposited in the fuel is calculated for the ultimate power cases assuming adiabatic heat addition based on the power transient from the point kinetics results. In cases where little or no DNB occurs, this assumption results in greatly overestimating the peak fuel enthalpy, and in all cases the value will be high. The calculation of the peak fuel enthalpy depends only on the power shape and the curve of peaking factors as a function of core volume. The peaking factors used result in higher peak enthalpies than would result from a calculation based on the peaking factors from a 1-dimensional space-time calculation. The space-time calculation is used as a check on the point kinetics results to ensure conservatism in the hot pellet fuel enthalpies. This check method has been discussed in the Oconee PSAR, Supplement 2, Question 6.2 (Dockets 50-269 and -270). A typical power transient from the space-time calculation is shown in Figure 14A.25-1 for a rod worth of  $0.49\% \Delta k/k$  which is greater than the maximum available. The initial power depression, peak power shape, and the steady state power shape with the rod removed (normalized to the peak power) are shown.

As a further demonstration of the sensitivity of the peak enthalpy to the major kinetics parameters, a detailed parameter study has been done as described in 14.2.2.2. This sensitivity analysis included the effects of varying the Doppler and moderator coefficients, rod worth and trip delay time. These analyses show that variations in these parameters cause little change in the heat addition.

0212

~~00123~~

QUESTION 14A.26 How is spatial dependence treated for  $\beta_{\text{eff}}$ ,  $k_{\infty}$ ,  $l^*$ ? Evaluate the uncertainty in peak power densities associated with this (DRL 14.7) approach.

ANSWER The  $\beta$ (effective) is input in the 1-dimensional, space-time kinetics code as a function of position. To obtain high worth rods in the core at EOL, nearly fresh (unpoisoned) fuel had to be simulated. This fuel would have a relatively high value for  $\beta$ , but the actual EOL  $\beta$  was input. This indicates that for a region of high burnup fuel, the rod worth would necessarily be much less than that used. The properties that go into the calculation of the infinite multiplication factor and the neutron generation time are also input as functions of position. It is therefore expected that very little uncertainty exists in the peak power densities because of this approach, except that the rod worths used are too high, which will increase the energy deposition. Figure 14A.26-1 shows the results of varying  $\beta$  around the value calculated for EOL conditions. For example, a  $\beta$  of 0.004 (Question 14A.24) causes a peak enthalpy of about 179 cal/gm which is still 101 cal/gm below the threshold for release of fuel to the reactor coolant.

~~00127~~

0213

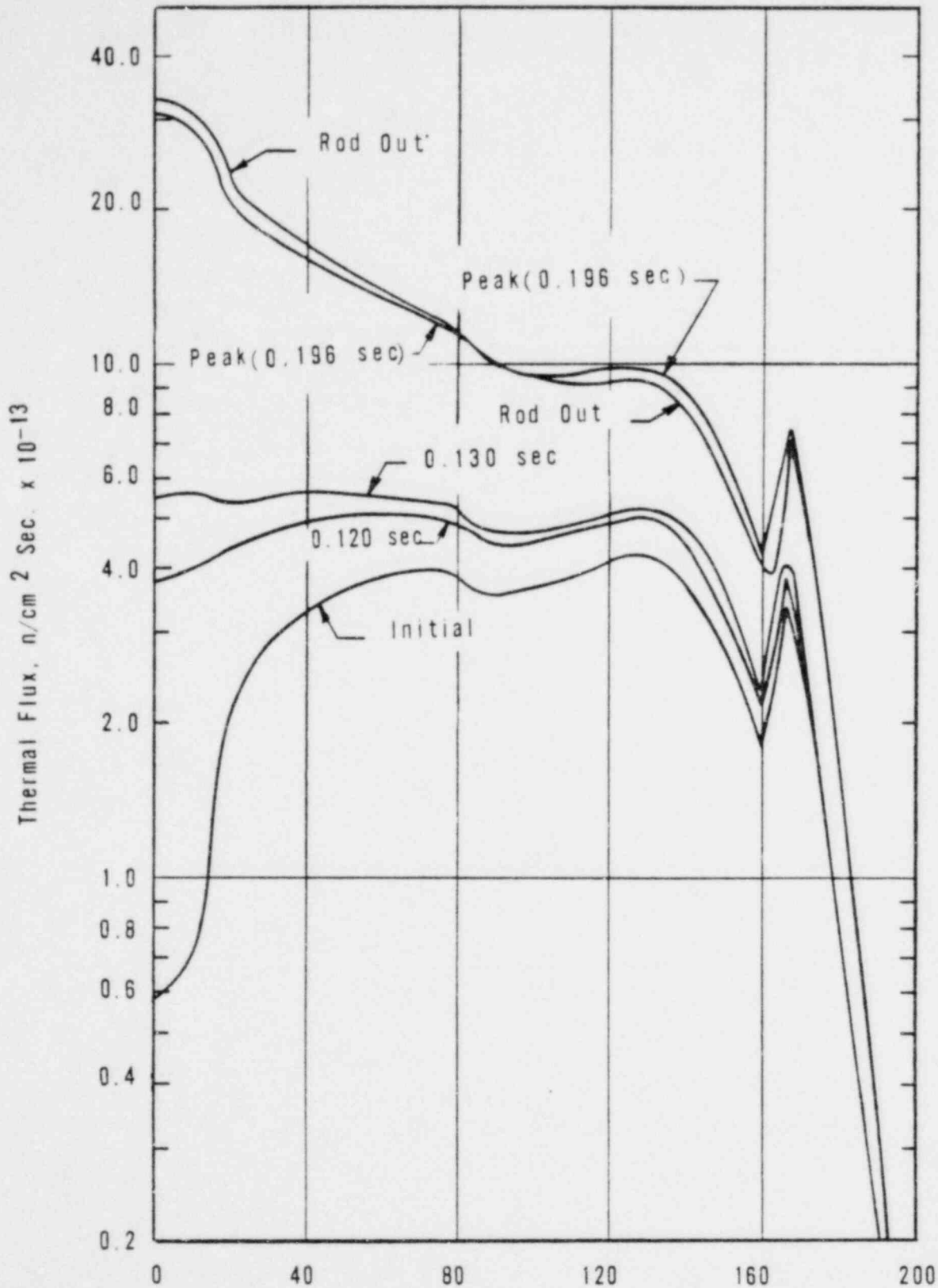


FIGURE 14A.25-1  
 THERMAL NEUTRON FLUX VERSUS  
 CORE RADIUS BEFORE AND DURING  
 A 0.49%  $\Delta k/k$  ROD EJECTION

0214

~~00130~~



**SMUD**

SACRAMENTO MUNICIPAL UTILITY DISTRICT

Peak Enthalpy For Hottest Fuel Pellet, cal/gm

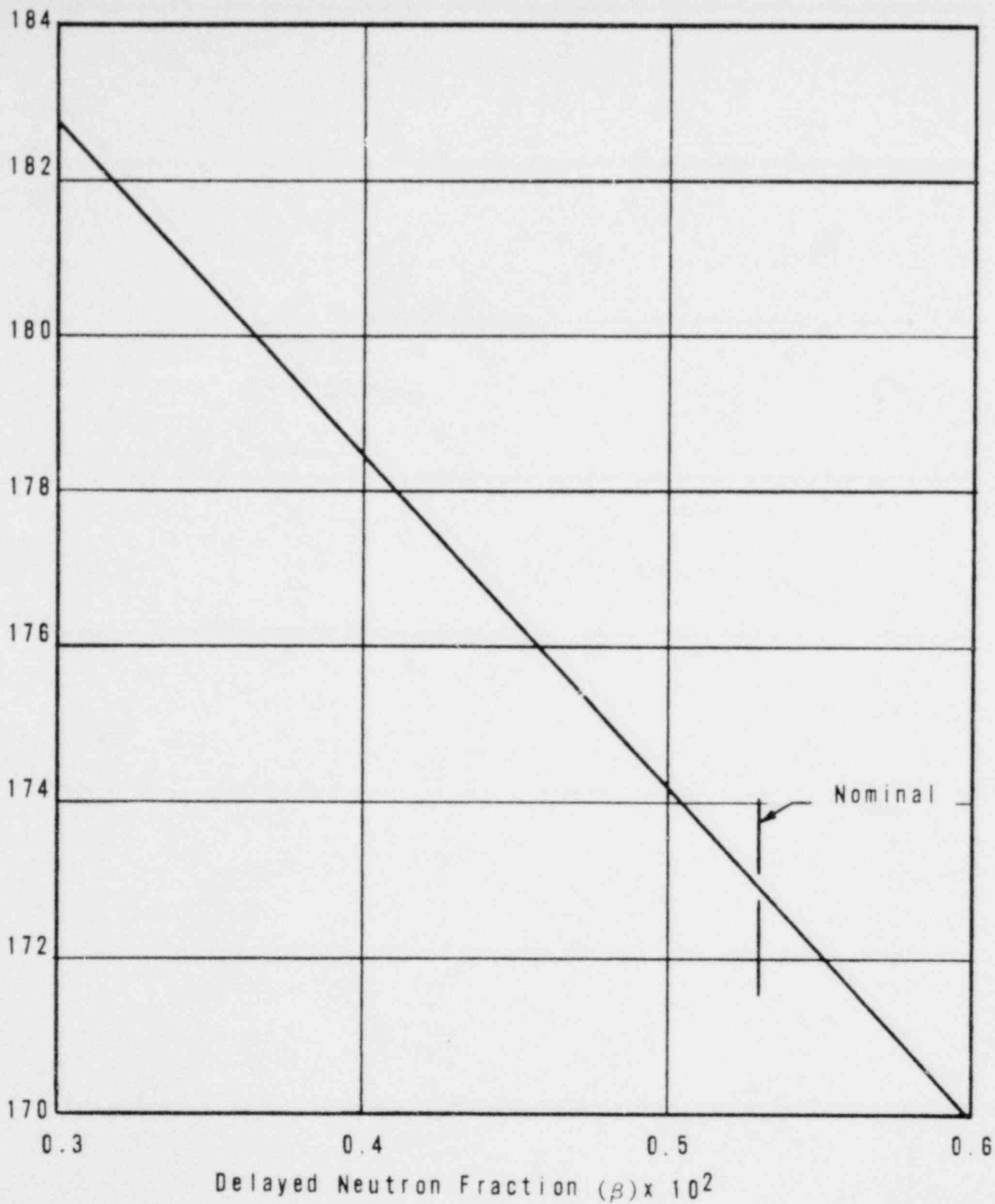


FIGURE 14A.26-1  
PEAK ENTHALPY OF THE HOTTEST FUEL PELLET  
AS A FUNCTION OF THE TOTAL EFFECTIVE  
DELAYED NEUTRON FRACTION FOR A 0.46%  $\Delta k/k$   
ROD EJECTION FROM ULTIMATE POWER AT EOL

0215



**SMUD**

SACRAMENTO MUNICIPAL UTILITY DISTRICT

~~00131~~

Amendment 2

QUESTION Provide the following results of your analysis of the load loss  
14A.21 transient.

(DRL 14.2)

- (a) Rise in average moderator temperature
- (b) Minimum DNB ratio during the transient
- (c) Rise in reactor loop pressures
- (d) Extent of turbine overspeed
- (e) The reactor thermal power transient
- (f) Fuel and clad temperatures.

ANSWER

Figures 14A.21-1 through 14A.21-4 show average moderator temperature, system pressure, reactor thermal power, and fuel average temperature and clad average temperatures for a typical loss of load transient. These data are based on a turbine trip from full load. The moderator coefficient of reactivity is taken as zero for these set of data.

DNBR data is not presently available for this transient. While this transient is a turbine trip, the load rejection transient is similar for approximately the first minute of the transient. In the load rejection transient the turbine overspeeds to 106% to 109% of normal speed during the first 40 to 60 seconds of the transient. When the turbine speed returns to normal, the intercept and control valves open to control electrical load. Turbine speed is on governor control at this time.

~~00132~~

0216



QUESTION 14A.22 Describe the natural circulation characteristics of the primary loop system. Will operation of primary loop relief valves, due (DRL 14.3) to its deadband characteristics, affect this flow?

ANSWER Figure 14A.22-1 shows the natural circulation flow characteristics of the reactor coolant system as a function of power level.

It is not expected that the deadband characteristics of primary loop relief valves will affect natural circulation flow because after natural circulation flow has commenced primary system pressure will remain below the set point for actuation of primary loop relief valves.

3

QUESTION 14A.23 In Figures 14.2.1 through 14.2.11 of the PSAR, the reactor kinetic parameters are given for  $\alpha_d$ ,  $\alpha_M$ ,  $l^*$  and  $\tau$ . What were (DRL 14.4) the corresponding values for  $\beta_{eff}$ ?

ANSWER The value for  $\beta$ (effective) for BOL is 0.0071 and for EOL is 0.0053.

QUESTION 14A.24 Discuss the technique used in calculating the effective delayed neutron fraction and include a summary of your calculations for (DRL 14.5) the end-of-life value.

ANSWER In calculating the  $\beta_{eff}$  of the design core, the values found in Table 1-16, ANL-5800 Second Edition were used.

The  $\beta$  for each fissionable isotope was weighted by the power produced by that isotope over the core. The power fractions were taken from a one-dimensional radial lifetime calculation.  $\beta_{eff}$  was calculated for BOL and EOL of cycle I and EOL of cycle IV.

BOL Cycle I  $\beta_{eff}$  = .0071

EOL Cycle I = .0057

EOL Cycle IV = .0053

Although the minimum value for  $\beta_{eff}$  is calculated to be 0.0053 for the core with a maximum burnup, the analysis of the rod ejection accident has been done for values of  $\beta_{eff}$  ranging down to 0.0030.

0217

An additional evaluation of  $\beta_{eff}$  has been completed using the following scheme.

- (1) Calculate the delayed neutron fraction at birth energies.
- (2) Consider the effect of prompt neutrons being born at higher energy than the delayed neutrons and having a greater chance of undergoing fast leakage and fast fission than one lower energy delayed neutrons.

- (1) In calculating  $\beta$  the maximum number of fissions from plutonium was assumed. The table below shows  $\beta$  for each isotope and the fraction of power from each isotope.

<u>Nuclide</u>	<u><math>\beta</math></u>	<u>% Power</u>
U-235	.0065	28%
U-238	.0157 (fast fission)	7%
Pu-239	.0021	65%

$$\beta = \beta^{35} (\% \text{ power})^{35} + \beta^{38} (\% \text{ power})^{39} + \beta^{39} (\% \text{ power})^{38}$$

$$\beta = .0043$$

$$(2) \quad \beta_{eff} \approx \beta \left[ \frac{\epsilon_D}{\epsilon_P} \cdot \frac{1 + T_P B^2}{1 + T_D B^2} \right]$$

$$\approx 0.004$$

This newer treatment was done for the fuel which has experienced the maximum allowable burnup. This fuel would never occur in the core in large quantities by itself, but would always be surrounded by fuel with much less burnup, therefore this result does not represent a macroscopic parameter as used in any safety analysis, but rather a minimum below which no part of the fuel would ever operate.

This minimum value of  $\beta_{eff}$  is still much larger than that considered in the rod ejection accident analysis.

0218

~~00134~~

QUESTION 14A.25 Discuss the accuracy of the energy yield predictions for the rod ejection accident. Your discussion should include the (DRL 14.6) anticipated power profile transients.

ANSWER The energy deposited in the fuel is calculated for the ultimate power cases assuming adiabatic heat addition based on the power transient from the point kinetics results. In cases where little or no DNB occurs, this assumption results in greatly overestimating the peak fuel enthalpy, and in all cases the value will be high. The calculation of the peak fuel enthalpy depends only on the power shape and the curve of peaking factors as a function of core volume. The peaking factors used result in higher peak enthalpies than would result from a calculation based on the peaking factors from a 1-dimensional space-time calculation. The space-time calculation is used as a check on the point kinetics results to ensure conservatism in the hot pellet fuel enthalpies. This check method has been discussed in the Oconee PSAR, Supplement 2, Question 6.2 (Dockets 50-269 and -270). A typical power transient from the space-time calculation is shown in Figure 14A.25-1 for a rod worth of 0.49%  $\Delta k/k$  which is greater than the maximum available. The initial power depression, peak power shape, and the steady state power shape with the rod removed (normalized to the peak power) are shown.

As a further demonstration of the sensitivity of the peak enthalpy to the major kinetics parameters, a detailed parameter study has been done as described in 14.2.2.2. This sensitivity analysis included the effects of varying the Doppler and moderator coefficients, rod worth and trip delay time. These analyses show that variations in these parameters cause little change in the heat addition.

0219

~~00155~~

QUESTION 14A.26 How is spatial dependence treated for  $\beta_{\text{eff}}$ ,  $k_{\infty}$ ,  $l^*$ ? Evaluate the uncertainty in peak power densities associated with this (DRL 14.7) approach.

ANSWER The  $\beta$ (effective) is input in the 1-dimensional, space-time kinetics code as a function of position. To obtain high worth rods in the core at EOL, nearly fresh (unpoisoned) fuel had to be simulated. This fuel would have a relatively high value for  $\beta$ , but the actual EOL  $\beta$  was input. This indicates that for a region of high burnup fuel, the rod worth would necessarily be much less than that used. The properties that go into the calculation of the infinite multiplication factor and the neutron generation time are also input as functions of position. It is therefore expected that very little uncertainty exists in the peak power densities because of this approach, except that the rod worths used are too high, which will increase the energy deposition. Figure 14A.26-1 shows the results of varying  $\beta$  around the value calculated for EOL conditions. For example, a  $\beta$  of 0.004 (Question 14A.24) causes a peak enthalpy of about 179 cal/gm which is still 101 cal/gm below the threshold for release of fuel to the reactor coolant.

~~00136~~

0220

QUESTION 14A.27 For the rod ejection accident (Section 14.2.2.2 of the PSAR), discuss the predicted pressure pulse in the reactor vessel and (DRL 14.8) the associated uncertainties.

ANSWER The reactor vessel capability has been analyzed to estimate the margin that exists between the calculated rod ejection transients and those that could initiate reactor coolant system failure. The pressure vessel material is SA-302 grade B steel. The material properties and equivalent sizes are given in the following table.

Yield strength (0.2% offset), psi	55,000
Ultimate strength, psi	80,000
Ultimate strain ( $\epsilon_u$ ), %	26
Strain energy ( $E_s$ ) per unit volume up to one-half the ultimate strain, in.-lb/in <sup>3</sup>	8,000
OD, in.	188.25
ID, in.	166.69
Thickness, in.	10.78

The radial deformation that will be assumed to represent failure of the vessel is 50% of the total elongation; i.e., 0.13 in/in.

To calculate the weight of an explosive charge required to reach 50% elongation, the vessel was simulated by a single cylinder with the same OD as the vessel but with an increased thickness to account for the thermal shield and core barrel. This equivalent thickness is the sum of the vessel thickness (8.44") and weighted thickness of the thermal shield (2.0") and core barrel (1.75") using the strain energy of 50% of the total strain.

The expression for the weight of an explosive charge required to strain the vessel a given amount is<sup>1</sup>

$$W = \left[ \frac{1.407 E_s (3.41 + 0.117 R_i/t) (R_e^2 - R_i^2)^{1.85}}{10^5 w^{-0.85} (1.47 + 0.0373 R_i/t)^{0.15} R_i^{0.15}} \right]^{0.811}$$

where  $W$  = charge weight (TNT or pentolite), lb.

$w$  = weight density of vessel material, lb/ft<sup>3</sup>

$R_i$  = initial internal radius of vessel, ft.

$R_e$  = initial external radius of vessel, ft.

$t$  = initial wall thickness of vessel wall, ft.

$E_s$  = wall strain energy, in.-lb/in.<sup>3</sup>

0221

Using this expression on the equivalent vessel, the required weight of explosive charge is 1410 lb of TNT to strain the mid-meridian ring up to 50%  $\epsilon_u$ . This quantity of explosive has an energy equivalent of  $6.74 \times 10^8$  cal.

An analysis has been made for high ejected rod worths than in 14.2.2.2 to estimate the transient required to generate the deformation energy equivalent to 1410 lb of TNT. The amount of zirconium-water reaction was determined and the heat resulting therefrom. The amount of fuel melting was also calculated and the assumption made that the fuel which exceeds the melting threshold is fragmented and dispersed into the coolant and quenched to the coolant average temperature.

The conversion of this rapid thermal energy release to an equivalent deformation energy is dependent upon the duration of the energy release. TNT has an energy release in microseconds and has a deformation energy conversion efficiency of only 50%. Therefore, only  $3.37 \times 10^8$  cal is available as deformation energy. The energy generated during a reactor transient from zirconium-water reaction and a molten fuel dispersal is not released in microseconds, but in second to millisecond time periods. Thus the conversion efficiency of thermal to deformation energy is low compared to TNT. Based on test data<sup>2</sup>, this conversion efficiency is less than 1/5 that experienced with TNT. Using this conversion, a reactivity addition of about 1.90%  $\Delta k/k$  is within the reactor vessel capability. Thus the reactivity addition required to produce possible damage to the reactor coolant system is about four times the maximum rod worth available.

#### REFERENCES

- <sup>1</sup> Wise, W. R., Jr. and Proctor, J. F., Explosion Containment Laws for Nuclear Reactor Vessels, NOLTR 63-140, Aug. 1965.
- <sup>2</sup> Wise, W. R., Jr. An Investigation of Strain Energy Absorption Potential as the Criterion for Determining Optimum Reactor Vessel Containment Design, NAVORD Report 5748, June 1958.

0222

~~00130~~

QUESTION 14A.28 (DRL 14.9) Discuss the potential for reactivity insertion and the associated consequences when a repaired pump is returned to service.

ANSWER The pump control circuitry will have an interlock to prevent starting an idle pump if the power level is above 15% of rated power. However, with three pumps running, it is possible to operate up to 75% rated power.

Assuming that three pumps are operating and the plant is at 75% of rated power, suddenly turning on the fourth pump will gradually reduce the average reactor inlet temperature as the pump comes up to speed. The maximum temperature decrease occurs after one loop time and amounts to about 13F. If a negative moderator temperature coefficient exists, this temperature change will cause a positive reactivity addition, which will increase the power level until the Doppler effect terminates the rise. If no automatic controls are used, this will cause a power mismatch between the reactor and steam generator which will increase the temperature and pressure in the reactor coolant system.

The results of an analog computer simulation without automatic control show that the cooler water circulating in the system will cause the neutron power to just reach the trip point at 114% of rated power on the second pass through the core. The pressure also reaches the trip point about 2 seconds later.

At lower initial powers, the temperature decrease is less severe and the neutron power will only increase several percent. However, the power unbalance will increase the pressure to the trip point. The use of automatic controls would readily compensate for the unbalance and the pressure and temperature transients would be much smaller, which in turn would cause the reactor power to remain even closer to its initial level.

The reactor thermal power lags the neutron power and even for the 75% power case, it only peaks at 98% of rated power. Therefore no core damage will result from inadvertently starting a fourth reactor coolant pump when operating at up to 75% power.

0223

~~00139~~

QUESTION  
14A.29  
(DRL 16.2)

Discuss and evaluate your design changes that will provide the capability for prompt detection of gross failure of a fuel element.

ANSWER

No design changes are proposed to the present system.

Scoping studies are in progress. The first step will be to evaluate the fission product activity levels which would result with various percentages of fuel rods damaged. The second step of the study will be to determine the sensitivity of the present radiation monitoring system and to compare it with the activity levels determined in the first step of the study. The study should be completed by the end of 1968.

QUESTION  
14A.30  
(DRL 16.3)

Discuss and evaluate your program of analysis and design directed to assure that fuel failures will not significantly inhibit the ECCS from preventing clad melting.

ANSWER

A study of clad failure mechanisms associated with a loss-of-coolant accident is presently underway. This study has included identification of the potential failure mechanisms, a search of the literature to obtain applicable data, evaluation and application of existing data, and scoping tests to obtain data on potential failure mechanisms. The initial results of this study include the identification of the failure mechanisms, an evaluation of the information available in the literature concerning these mechanisms, and an evaluation of the effects of these mechanisms on the reactor system design.

The objective of the study is to insure that there are no potential failure mechanisms that might interfere with the ability of the emergency core cooling systems to terminate the core temperature transient and remove decay heat in the event of a loss-of-coolant accident. These potential failure mechanisms include clad melting, zirconium-water reaction, eutectic formation between the Zircaloy clad and the stainless steel spacer grids, the possibility of clad embrittlement as a result of the quenching during core flooding, and clad perforation or deformation accompanying its failure. In the case of clad melting and zirconium-water reaction, the present design limit for peak clad temperature precludes these as possible failure modes. Information available in the literature along with experimental evidence from tests conducted by B & W show that brittle fracture of the cladding will not occur as a result of quenching following a loss-of-coolant accident, and that eutectic formation between dissimilar core materials will not interfere with the flow of emergency core coolant after the accident.

~~00140~~



Many of the fuel rods may be expected to experience cladding perforation during the heatup in the loss-of-coolant accident as a result of fission gas internal pressure and weakening of the clad as its temperature increases. The mechanical strength of Zircaloy cladding is reduced as the temperature exceeds 1,000F, so that the fuel rods with appreciable fission gas internal pressure will begin to fail locally and relieve the gas pressure when the temperature exceeds 1,100F. Some local deformation of the rods will occur before perforation. However, cooling would still be effective, since the fuel rods are submerged, and cross-channel flow around the ballooned area will cool the rod. At worst a local hot spot may occur.

To verify that the perforation/deformation failure mode will not significantly inhibit the emergency core cooling system from preventing clad melting, B&W has undertaken a program to evaluate in detail the effects of perforation and deformation of fuel rods during the temperature transient following the loss-of-coolant accident. Preliminary tests have been run on nine samples of Zircaloy-4 cladding filled with ceramic pellets, and additional experiments are planned to gain a clearer understanding of the effects of temperature excursions on Zircaloy-clad fuel elements. Current plans include performance of a three-phase program. In the first two phases, which are experimental, single-rod excursions will be performed to better establish temperature-pressure relationships at the time of clad perforation. The single rod tests of the first phase will also investigate the extent of deformation to be expected under the varying conditions associated with simulated in reactor temperature excursions. These will include the effects of hydrogen concentration and oxide films. The second phase of the program will consist principally of multi-rod tests to explore the effect of the restraining action of spacer grids and adjacent fuel rods and to determine the randomization of the localized deformation in an assembly of fuel rods. In the third phase of the program the data obtained from the two experimental phases will be applied to the analysis of the effects in a loss-of-coolant accident.

This program for the evaluation of the effects of perforation and deformation of fuel rods, including the analysis and application of the data obtained, is scheduled for completion by late 1969.